Force Reconstruction from Ejection Tests of Aircraft Stores Used for Model Predictions and Missing/Bad Gages

Michael R. Ross[1] and Michael J. Starr[2] and Angel Urbina[3] and Jerry Cap[4] and Adam Brink[5]
Sandia National Laboratories, Albuquerque, NM, 87106, USA

One of the more severe environments for a store on an aircraft is during the ejection of the store. During this environment it is not possible to instrument all component responses, and it is also likely that some instruments may fail during the environment testing. This work provides a method for developing these responses from failed gages and uninstrumented locations. First, the forces observed by the store during the environment are reconstructed. A simple sampling method is used to reconstruct these forces given various parameters. Then, these forces are applied to a model to generate the component responses. Validation is performed on this methodology.

I. Introduction

During most field experiments, gages will fail due to various reasons. A method to provide lost gage responses is to develop a model of the system, then subject the model to the forces that the system observed during the field test. This requires first, an ability to reconstruct the forces, and second, the capability to develop a model of the system. Measuring forces can be difficult if not impossible to obtain during certain testing, for the various reasons such as space limitation, force location, and hardware constraints. An ejection test of a store from an aircraft is one of these tests where it is difficult to measure the actual forces during the event.

One of the more severe and design driver for any store on an aircraft is when the store is ejected from the aircraft. This is representative of a shock environment. It is possible to reconstruct the forces on the store during this environment. These forces can then be applied to various models to assess the weapons performance during this event. The force reconstruction requires measured acceleration responses during the environment, and a separate laboratory hammer tap test. The hammer tap test is used to develop transfer functions between force input locations to desired field measured responses.

Once the transfer function is developed, it in conjunction with the measure field/environment shock responses can be used to reconstruct forces observed by the store during the ejection shock. The forces can then be applied to a finite element model or a transfer function matrix to obtain other desired component locations responses either not measured during the field test or at a location where a gage as gone bad. This study builds on previous work done at Sandia National Laboratories with use of a simple sampling method and additional sensitivity studies to find a preferred set of gages to be used for the force reconstruction from a recent ejection test.

These reconstructed forces are then used to predict responses at three locations in each of the Cartesian directions, a total of nine gages that failed to work during the test. Excellent agreement is found with eight out of the nine gages, where the average error is less than 2 *dB*. It is believed that one particular gage had problems during the experiment to build the transfer function.

This report begins in Section IIA with a derivation of the theory for this force reconstruction given a field test and a laboratory hammer tap test. Section IIB discusses the actual experiments. Next, in Section IIC verification of the algorithms and the code used for this work is provided. There are several parameters that need to be explored to

---

[1] Principal Member Technical Staff, Program & Test Integration, P.O. Box 5800, Senior Member AIAA.
[2] Principal Member Technical Staff, Program & Test Integration, P.O. Box 5800.
[3] Principal Member Technical Staff, Program & Test Integration, P.O. Box 5800, Senior Member AIAA..
[4] Principal Member Technical Staff, Program & Test Integration, P.O. Box 5800.
[5] Senior Member Technical Staff, Structural Dynamics Department, P.O. Box 5800..

generate the best force reconstruction and this is discussed in Section IID. Once the force is reconstructed, Section III, provides an example of responses for missing field gages and provides a low frequency excitation. Section IV provides validation metrics between different ejection racks.

II. Ejection Force Reconstruction

This section ultimately provides a set of forces that are experienced on a store during an ejection event from the aircraft. These forces can then be applied to various models to assess the weapons performance during this event. To develop these forces requires the use of a laboratory hammer tap test and measured responses during the ejection test. This section also discusses the set of parameters that can be used to develop this force reconstruction. It was found that a simple sampling method could be used to find a respectable set of forces from various parameters.

A. Theory

The theory begins with an essential tool in linear dynamics, the Frequency Response Function (FRF). Fundamentally, a FRF express the responses/outputs of the system to an applied set of inputs as a function of frequency. The FRF is the ratio between the Fourier transforms of the responses and the Fourier transforms of the input excitations [1]. In this work, the response/output is noted as acceleration and the input is a force. In this particular case the FRF is sometimes noted as the *Accelerance*. Thus, the FRF, $[H(\omega)]$, is used to relate the input force, $\{F(\omega)\}$, to the output acceleration $\{A(\omega)\}$:

$$\{A(\omega)\} = [H(\omega)]\{F(\omega)\}. \tag{1}$$

If the acceleration responses are known from a field test (*field*) and the FRF has been computed from a different test, such as a laboratory hammer tap test (*ham*), then one can generate the required force that produced the set of accelerations from the following:

$$\{F(\omega)\}_{field} = [H(\omega)]_{ham}^{-\dagger} \{A(\omega)\}_{field}, \tag{2}$$

where †, is the Moore-Penrose pseudoinverse.

1. *Analysis Details*

There are several complicated issues with this simplified procedure. One important but often overlooked issue in this work is keeping track of the indices for the responses and the excitation locations. This is important for the formulation of the FRF matrix, $[H(\omega)]$, that has been provided from an experimental laboratory hammer tap test, discussed in Section IIB. Another challenging task is going between the time and frequency domains appropriately. This is done using the Fast Fourier Transform (FFT) and the Inverse Fast Fourier Transform (IFFT). These items have been verified and are discussed in Section IIC.

Once the FRF matrix, $[H(\omega)]$, has been formed it is then a matter of determining its inversion and multiplying by the desired acceleration response in the frequency domain. However, before the multiplication is performed the acceleration time history data is pre and post conditioned such that it begins and ends at zero with a smooth transition. This is accomplished by multiplying by the functions depicted in Figure 1 for the first and last $4x10^{-3}$ seconds (T_0). The functions are the following:

$$\text{Pre/Front Condition: } 1/2\left\{1 - \cos\left(\frac{\pi t}{T_0}\right)\right\} \tag{3}$$

$$\text{Post/Back Condition: } 1/2\left\{1 + \cos\left(\frac{\pi t}{T_0}\right)\right\}. \tag{4}$$

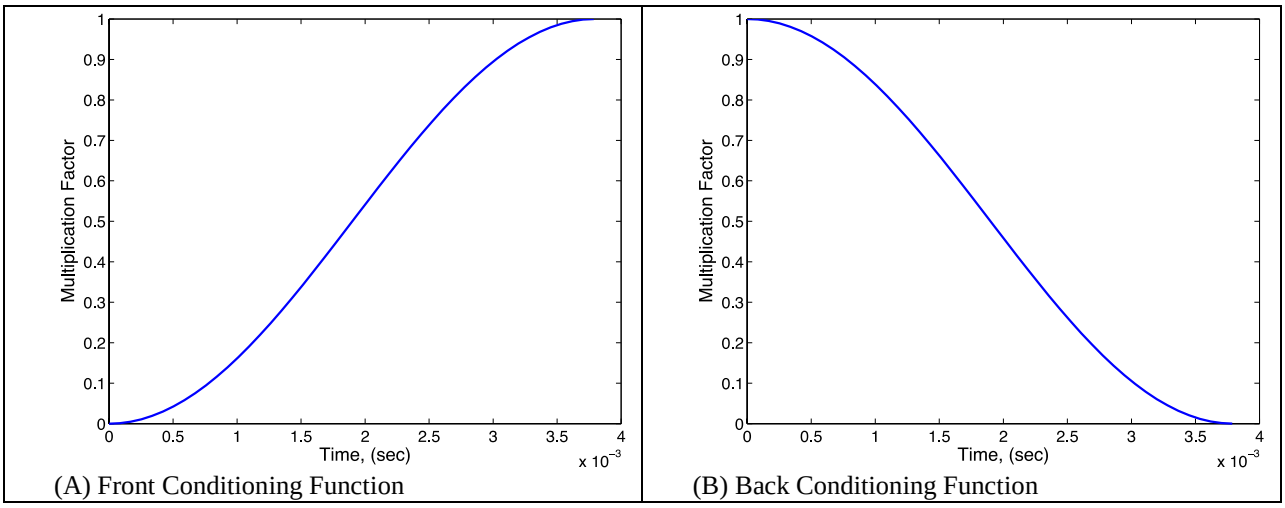

(A) Front Conditioning Function (B) Back Conditioning Function

Figure 1: Pre and Post conditioning functions to assure the acceleration data begins and ends a zero with a smooth transition.

In addition, before the multiplication of the $[H(\omega)]_{ham}^{-\dagger}\{A(\omega)\}_{field}$, is performed the $[H(\omega)]_{ham}^{-\dagger}$ is interpolated to be at the same frequency resolution as the acceleration $\{A(\omega)\}_{field}$. This is done because the Fourier transforms of the acceleration time vector is typically more frequency dense then the FRF matrix. For the forward problem, $\{A(\omega)\} = [H(\omega)]\{F(\omega)\}$, the same interpolation procedure is applied.

Another important item is the time duration for the analysis. Figure 2 depicts the time history at gage 635BZ. Gage 635BZ was a gage located on the aft section of a store during a recent ejection test. Time periods with very little response will cause numerical errors in the inversion and thus the time period explored is from 0.018 to 0.08 seconds.

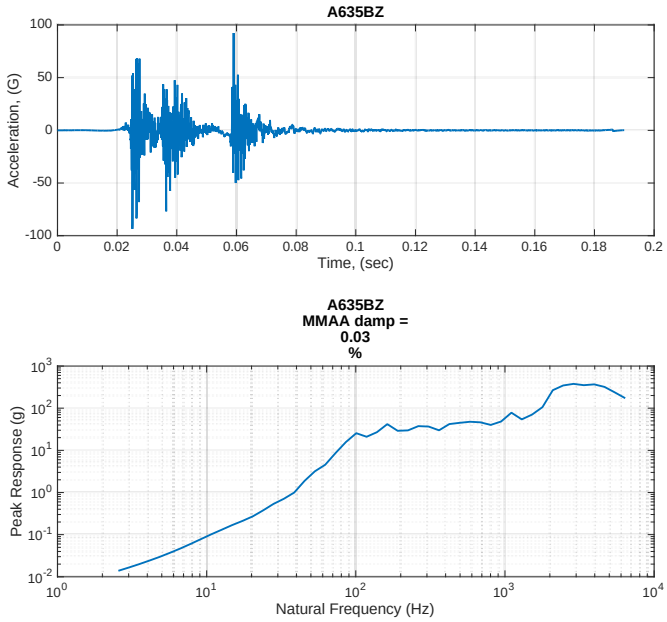

Figure 2: Time history and SRS for gage 635BZ, demonstrating the time period of the analysis should be around 0.018 to 0.08 seconds.

Finally, two more items need to be mentioned that where used in this study. First, the time history data is band-pass filtered from 60 to 6,000 *Hz*. Also, any gages that were not in system coordinates were removed from the list for the force reconstruction.

B. Experimental Set-up

There are two test required for this work. The first test is the "Hammer Tap Test" that is used to generate the FRF matrix. The second test is the actual "Ejection Test" where the desired force reconstruction is needed. The particular store used in this study has three main regions: the front, the body, and the tail. The body region has gages that are difficult to excite due to various damping mechanism within that region.

In both tests the Sandia Data Acquisition System (DAS) recorded all of the accelerometer channels. Each DAS channel consisted of an anti-aliasing filter (Precision Filter model 28314) and a 24-bit digitizer (VTI model VT1436). The accelerometer signals were lowpass filtered at 10 kHz using a Bessel filter and sampled the data at a rate of 25,600 samples / second.

The acceleration signals often contain low level offsets that do not go away with time. These anomalies, however small, can adversely bias the velocity and spectral analyses. Two steps were implemented to deal with this.

1) A segment of time from 20ms to 10ms prior to first motion was used to compute the mean "drift" acceleration. This mean drift was subtracted from the signal.

2) It is considered good practice to use the shortest time window possible (consistent with all of the channels for a given test ringing down) for the subsequent spectral analyses. This translates into a window from 3*ms* prior to first motion to 90*ms* after first motion.

1. Hammer Tap Test for FRF matrix Generation

The system was hung in a free-free configuration using two loops of one-inch thick bungee cord. A Hammer Tap test was conducted where input forces from the hammer taps and acceleration responses at various locations were recorded. This information and proper signal processing can generate the FRF matrix, $[H(\omega)]_{ham}$. There were eight hammer input locations: Forward Lug (FL), Aft Lug (AL), Forward Piston impact location (FP), Aft Piston impact location (AP), Forward Sway Brace on the positive Y side (FSBY+), Forward Sway Brace on the negative Y side (FSBY-), Aft Sway Brace on the positive Y side (ASBY+), and the Aft Sway Brace on the negative Y side (ASBY-). These are also listed in Table 1.

Table 1: Input happer tap force locations.

Abbreviation	Location
FL	Forward Lug
FP	Forward Piston
FSBY+	Forward Sway Brace on the Y+ Side
FSBY-	Forward Sway Brace on the Y- Side
ASBY+	Aft Sway Brace on the Y+ Side
ASBY-	Aft Sway Brace on the Y- Side
AP	Aft Piston
AL	Aft Lug

The FRF matrix is formed from the cross-spectral density between the response and excitation, $G_{af}(\omega)$, and the autospectral density of the excitation, $G_{ff}(\omega)$.

$$H(\omega) = \frac{G_{af}(\omega)}{G_{ff}(\omega)}. \tag{5}$$

2. Ejection Test

During the ejection testing the store is mounted on an ejection test frame and ejected within the laboratory. There is a foam pad used to provide a "soft catch" of the store after it has been eected. The ejection rack uses two

cartridges to generate the gas pressure needed to operate the rack's release and eject mechanism". The unit was ejected at three different temperature settings noted as ambient, cold, and hot.

For the ejection test there were some examples of relatively low frequency oscillatory drift, most notably in the aft end accelerometers. While the exact source of the anomaly is not known, the most probable sources of this type of behavior are 1) an intermittent cabling connection or 2) accelerometer grounding issues. Because this anomaly is often erratic in shape, it is difficult to remove analytically. Therefore, any signal exhibiting this type of anomaly was tagged as being "bad".

Piezoelectric accelerometers are susceptible to over ranging in severe shock environments. Two common sources of over ranging are 1) the saturation of the charge amplifier due to high frequency energy (in band or out of band), and 2) the depolarization of the piezoelectric crystal. Both of these anomalies tend to occur most often for accelerometers nearest to the souce. When this was noticed these gages were determined to have failed.

C. Analytical Verification

Verification is the process of determining that a model implementation accurately represents the developer's conceptual description of the model and the solution to the model [2]. In this work, a model is built from a FRF that was developed during a hammer tap test. Given a set of acceleration responses, the model is then used to generate a force vector. This force vector can then be applied to the model to determine different gage response or can be applied to a completely different model, such as a finite element model, to predict other location responses or stresses in the model. It is imperative to have confidence in the process for generating the force vector. In an effort to build confidence in the force vector generation the following regression/unit tests are performed.

1. 125 Hz Sine Input Z-Direction

As a method to verify the implementation of the code, the first regression test consist of inputting a sine force function into the forward problem $\{A(\omega)\} = [H(\omega)]\{F(\omega)\}$, and obtaining acceleration response at a set of locations. With these the acceleration responses, the inverse problem is ran to obtain the force vector. A verification of the methodology is if the calculated force vector matches the test sine function force vector. The test input sine function is a frequency of 125 *Hz* with amplitude of 28,000 *lb*.

In order to test the implementation of the code, only Z-direction forces and responses are used. The force input location is thus chosen as the forward and aft lug, noted as *FL* and *AL* respectively, and the forward and aft piston impact location, noted as *FP* and *AP* respectively. Six response/acceleration locations are chosen throughout the system. The gage number is the following: 601BZ, 100BZ, 110BZ, 200BZ, 610BZ, 620BZ, and 625BZ. Thus, the $[H(\omega)]$ matrix is the size of *7,4,k*, where *k* is the number of frequency steps.

The first step in the verification process is assuring that the $[H(\omega)]$ matrix is of proper rank and well conditioned. This is performed throughout this study. In this particular regression test the $[H(\omega)]$ matrix should have a rank of four, this is shown in Figure 3. Figure 3 also shows that the FRF matrix is well conditioned. A large condition number is a good indicator of an ill-conditioned matrix. "As the condition number increases by a factor of 10; it is likely that one less digit of accuracy will be obtained in the solution" [3]. Generally, a double precision matrix provides 15 significant decimal digits precision [4]. Thus, a condition number of $1x10^{15}$ would indicate a singular matrix. In this study, any condition number below $1x10^{6}$ would be considered appropriate and better then single precision.

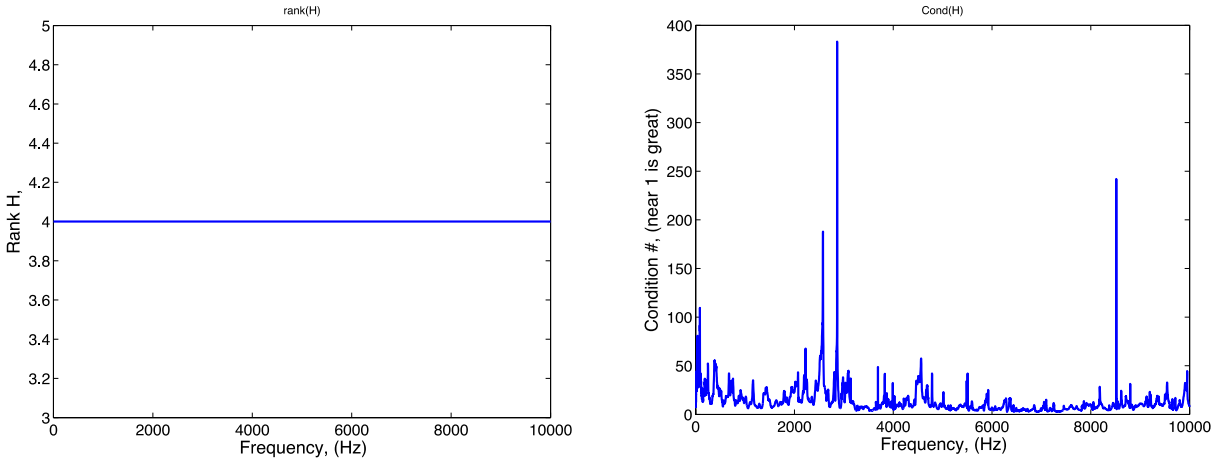

(A) Rank of the FRF matrix, H. (B) Conditioning of the FRF matrix, H.

Figure 3: Rank and Conditioning of the FRF matrix for the regression test of a sine input in the Z-direction.

As mentioned in Section A-1, the transfer function is provided in the frequency domain; however, it is desired to have the force in the time domain for the use with FE models. In addition, the acceleration responses from the Eject-1 test are provided in the time domain. Therefore, the algorithm and method for doing the Fast Fourier Transform (FFT) and the Inverse Fast Fourier Transform (IFFT) need to be verified as these are used frequently throughout this process. This is accomplished as shown in Figure 4, where the FFT produces the correct response for the 125 *Hz* sine input, and the IFFT of the FFT reproduces the original input sine function. In addition, during the FFT and IFFT, a check is in place to assure that the time vector and frequency vector are scaled correctly with use of Parseval's theorem.

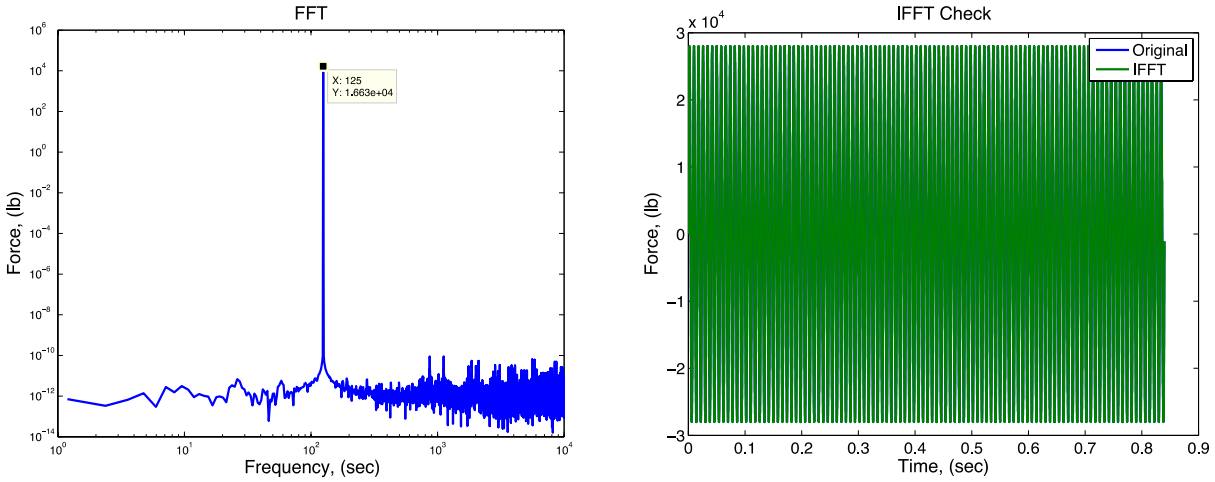

(A) FFT of the 125 Hz Sine Force Input. (B) Check that IFFT is calculated correctly.

Figure 4: Verification of FFT and IFFT.

The input force is then run in the forward direction to get the responses at the seven locations. The responses of the seven locations are then run through the algorithm for the inverse method to generate the forces. If the method is appropriately working, then the force from the inverse method should be the same as the test case force and this is shown for the force at the Aft Lug in Figure 5.

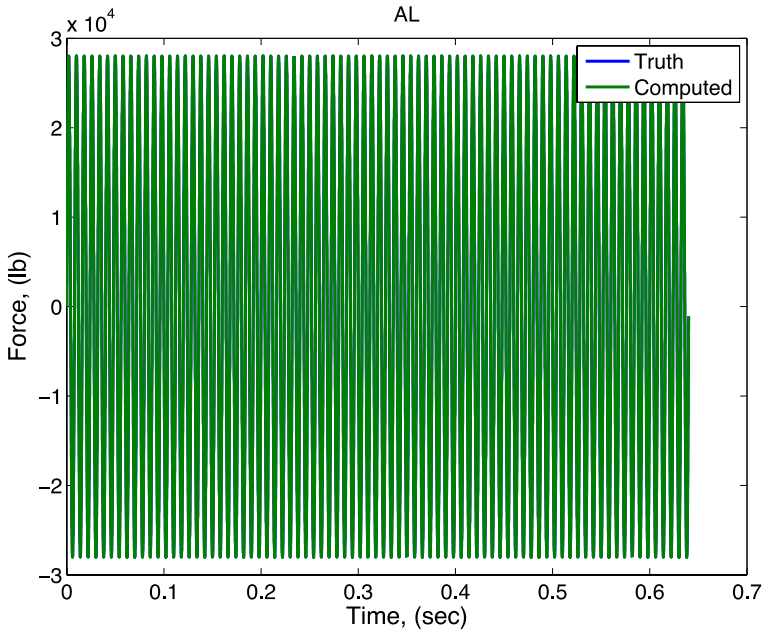

Figure 5: Comparison of Truth (Sine Test) Force function as compared to the Computed (inverse method).

2. 125 Hz Sine Input with Response in X and Y direction

For the first regression test, only the Z-direction input was originally tested. The response gages noted early were again used; however during this testing the *X* and *Y* response locations were used. The results were identical to that shown in Figure 5.

3. Two Sine Input Test with additional Force Locations

In order to further verify the code and give some fundamental understanding, two sine functions were superimposed to form the force vector. The two sine functions were at 125 *Hz* and 850 *Hz* with amplitude of 28,000 *lb*. An additional four more force input locations were used: the plus *Y* forward sway brace locations (FSBY+), the minus *Y* forward sway brace location (FSBY-), the plus *Y* aft sway brace location (ASBY+), and the minus *Y* aft sway brace location (ASBY-). This created a total of eight input locations.

At first, the previous seven responses were used to create the $[H(\omega)]$ matrix that is 7,8,k, with a Rank of seven. This produced a comparison between the truth inputs at the aft piston (AP) with the computed using the inverse method as shown in Figure 6. In Figure 6 there is an obvious error that is caused by using a lesser number of response locations as compared to the force inputs. This is a known issue with the inverse method and a simple correction is to use more response locations then desired force locations. Figure 7 shows the correct computed value at the forward piston (FP) when more response locations are used then desired force locations. In that figure the previous gages where used plus the *Y* direction of those gages for a total of fourteen response/accelerations and eight force input locations.

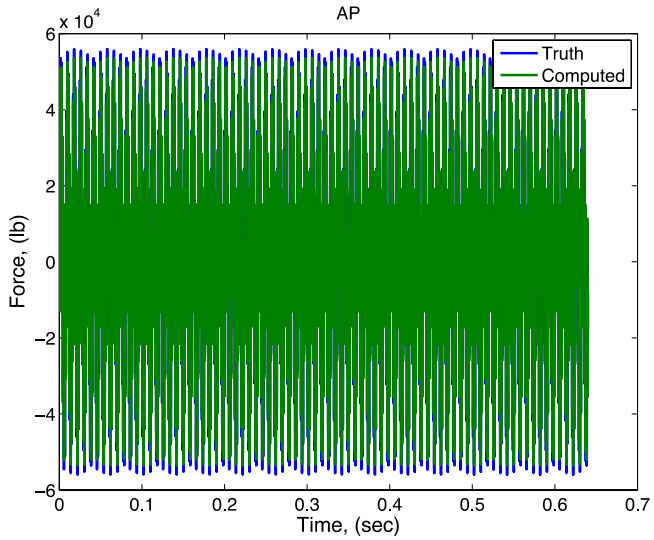

Figure 6: An example where there are fewer response locations then force inputs.

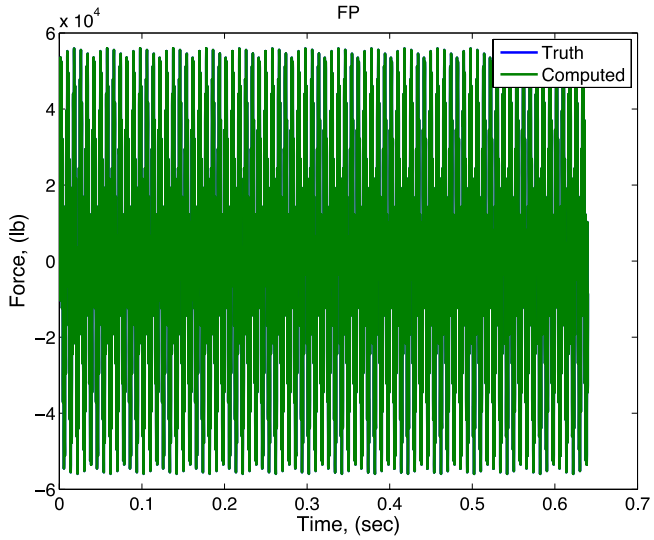

Figure 7: Illustration of using more response locations then force inputs proper inverse methodology.

4. Two Sine Inputs with Testing of Interpolation

In the previous regression tests, the frequency of the input sine was aligned with the frequency steps of the transfer function from the hammer tap test. The frequency steps in the hammer tap test were evenly spaced at 1.5625 *Hz.* This regression test examines the effect of the two sine inputs at different frequencies than the transfer function spacing. In this particular example, the sine frequency was slightly shifted to 130 Hz and 855 *Hz.* This produces correct results as similar to those shown in Figure 7 as long as the frequency resolution of the FFT and IFFT are the same spacing as the FRF. However, when the frequency resolution of the FFT and IFFT are different than the FRF spacing, then there will be some numerical error introduced during the interpolation of the FRF matrix to the frequency resolution from the FFT of the acceleration. As an example, if the frequency spacing for the FFT is 2.2727 *Hz* and the frequency resolution of the FRF remains at 1.5625 *Hz* then there is a slight numerical error introduced as seen in Figure 8 for the aft piston force input location.

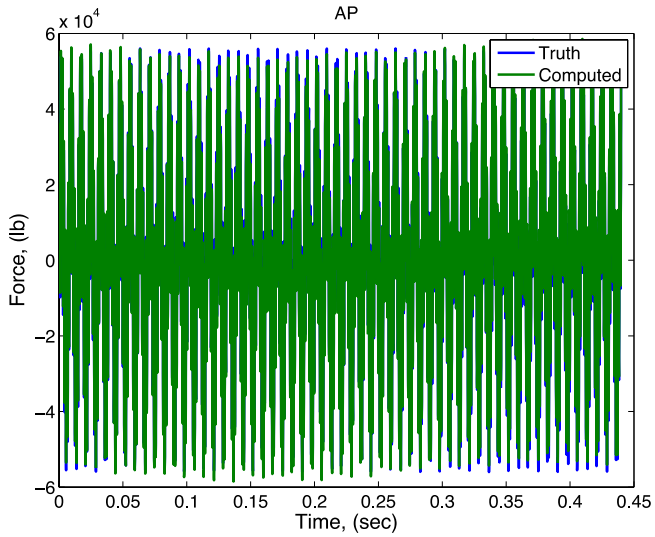

Figure 8: Slight numerical error introduced due to interpolating the FRF matrix to the frequency resolution of the FFT of the acceleration.

5. Haversine Input Regression Test

Given the previous lessons, a haversine input was used to test the algorithm as well. This produced similar results to the previous sections. As long as the previous lessons were adhered to then the computed produced an identical value to the truth as seen in Figure 9.

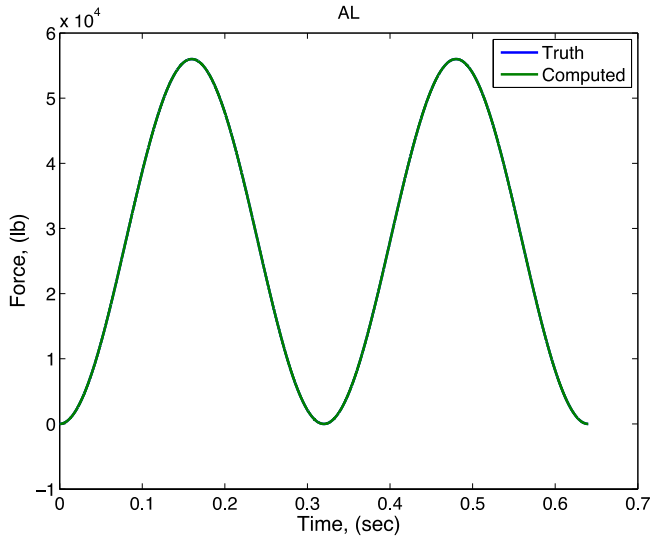

Figure 9: Haversine input regression test comparison.

D. Parameters for force reconstructions

There are several parameters that can be used for the force reconstruction. This section discusses the sensitivity studies performed to try and find an adequate set for use in reconstructing the force input vectors. There are three main comparisons done in the sensitivity study:

1. The first will be referred to as the *same gage* comparison. In the *same gage* comparison, the gages that are used to generate the force vector in the inverse problem, $\{F(\omega)\}_{field1} = [H(\omega)]_{ham}^{-\dagger}\{A(\omega)\}_{field1}$, are then the same gages that are compared to test data with the problem run in the forward manner $\{A(\omega)\}_{field1} = [H(\omega)]_{ham}\{F(\omega)\}_{field1}$.

2. The second comparison will be referred to as *opposite gage* comparison. In the *opposite gage comparison* a set of gages (*field1*) are used to generate the force vector in the inverse problem: $\{F(\omega)\}_{field1} = [H(\omega)]_{ham}^{-\dagger} \{A(\omega)\}_{field1}$. A set of *opposite gages* are found from the total set of gages (except any bad gages found) minus the *field1* gages used for the force generation. The force vector $\{F(\omega)\}_{field1}$, is then used to find the opposite gages responses in the forward direction: $\{A(\omega)\}_{opposite} = [H(\omega)]_{ham}\{F(\omega)\}_{field1}$.
3. Finally, the third comparison will be referred to as *check list*. In this comparison, a set of gages is predetermined for comparisons to test data. The optimal combination of test response gages is sought that minimizes the error between the test data and this predetermined set of gages. The predetermined sets of gages are listed in Table 2. This set of gages was determined by their location in the system and certain attributes of the responses that were desired to capture. The gage '610BX' was noted to have concerns during hot and cold ejection tests and was not used in the *check list*.

Table 2: *Check List* gages used for comparison with test data.

***Check List* Gages**			
110BX	460BX	635BX	610BY
110BY	460BY	635BY	610BZ
110BZ	460BZ	635BZ	

In order to find a satisfactory set of parameters for the force construction, a set of metrics needs to be determined. The actual environment and field test are representative of a shock. Though, there have been several methods proposed to assess the severity of shock [5] [6], this study uses the classic shock response spectra (SRS) originated by Biot [7] and formulated with the maximax absolute-acceleration (MMAA) with 3% damping [1]. In comparing two different SRS, such has from a test and an analysis; the 1/6th octave decibel error (*dB*) is computed. On each 1/6th octave center frequency the error is found as

$$dB_{error} = 20 * \log\left(\frac{SRS_{anal}}{SRS_{test}}\right). \tag{6}$$

Here a 6 *dB* difference means the higher value is twice as large as the lower value.

A baseline set of acceleration response gages and force input locations were predetermined to begin the comparisons and sensitivity studies. The selection of the baseline gages and force input locations began with the desire to use only locations in the Z direction, since this is the primary excitation axis of the field test. This limits the input locations to the two lug locations and the two piston locations. At least four response locations were necessary to keep the FRF matrix of sufficient rank. The combination of the following four gages: 601BZ, 100BZ, 110BZ, and 300BZ, produced a mean error of -0.1 *dB* and the maximum absolute error across 1/6th octave frequencies of 3.6 *dB* when using the *same gage* comparison method. The comparisons for each gage are shown in Figure 10 - Figure 13.

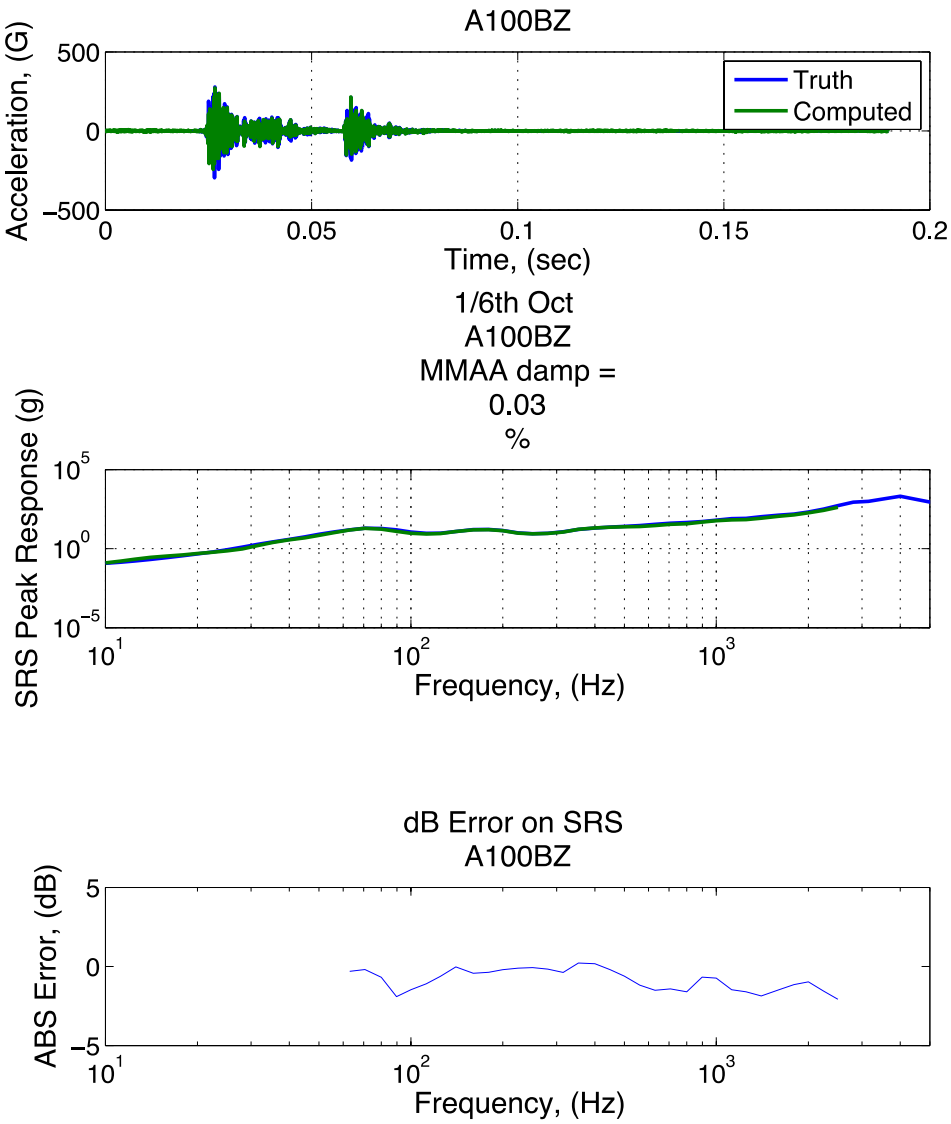

Figure 10: *Same Gage* comparison for gage 100BZ using the baseline set of gages.

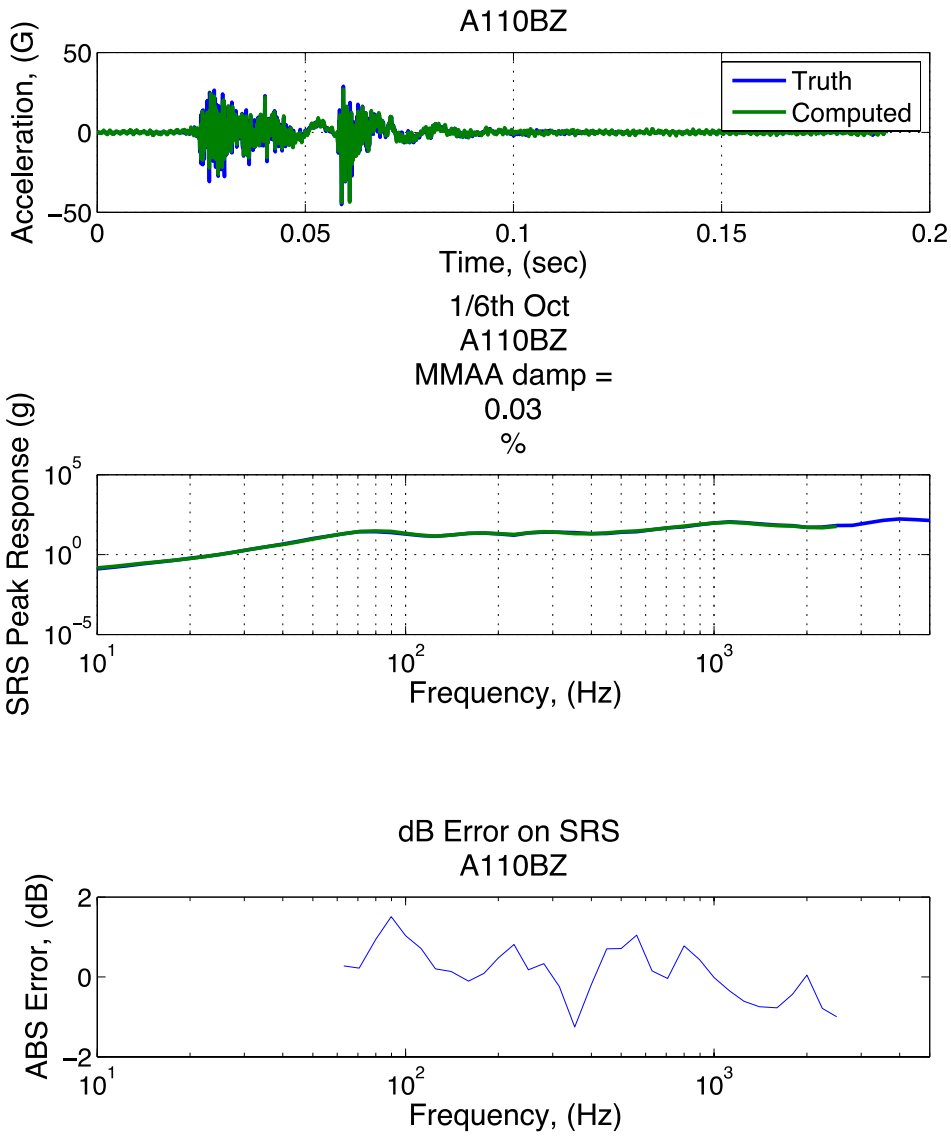

Figure 11: *Same Gage* comparison for gage 110BZ using the baseline set of gages.

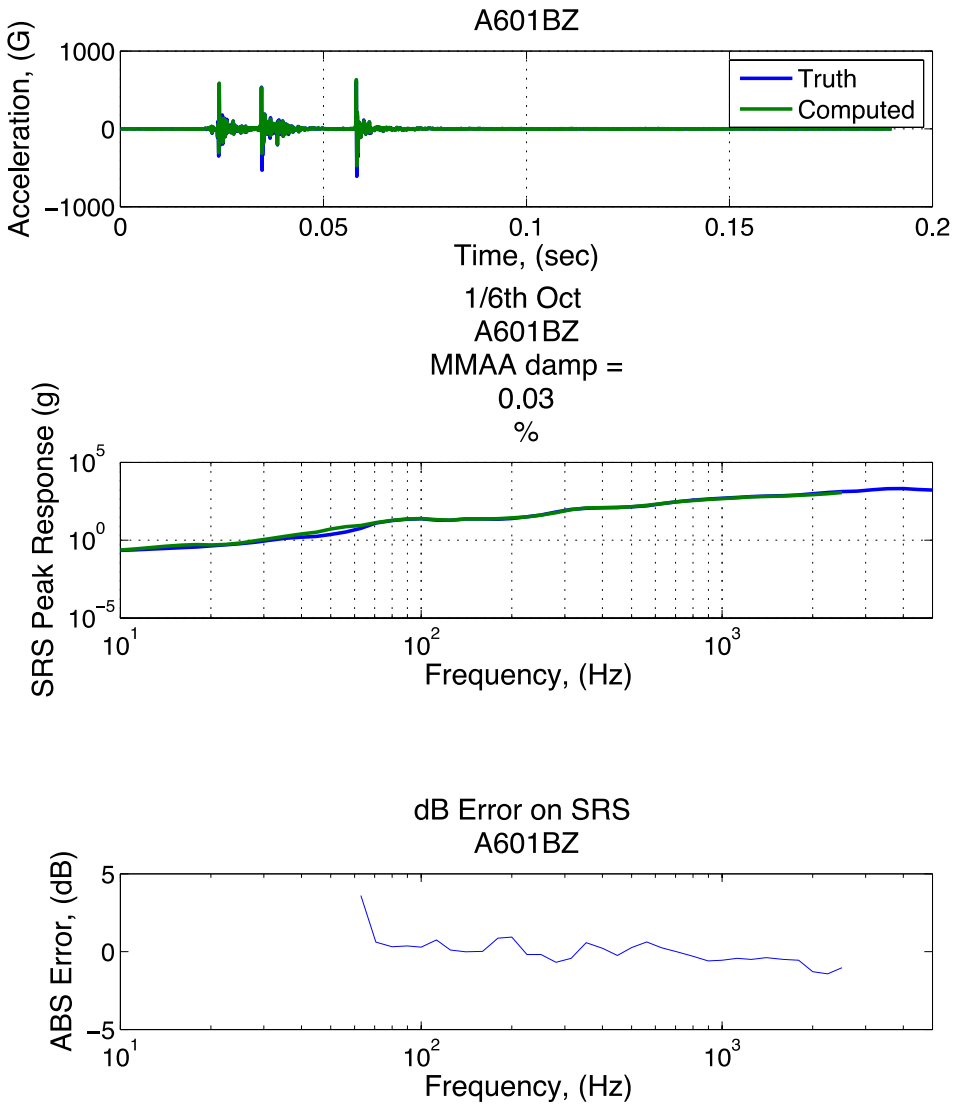

Figure 12: *Same Gage* comparison for gage 601BZ using the baseline set of gages.

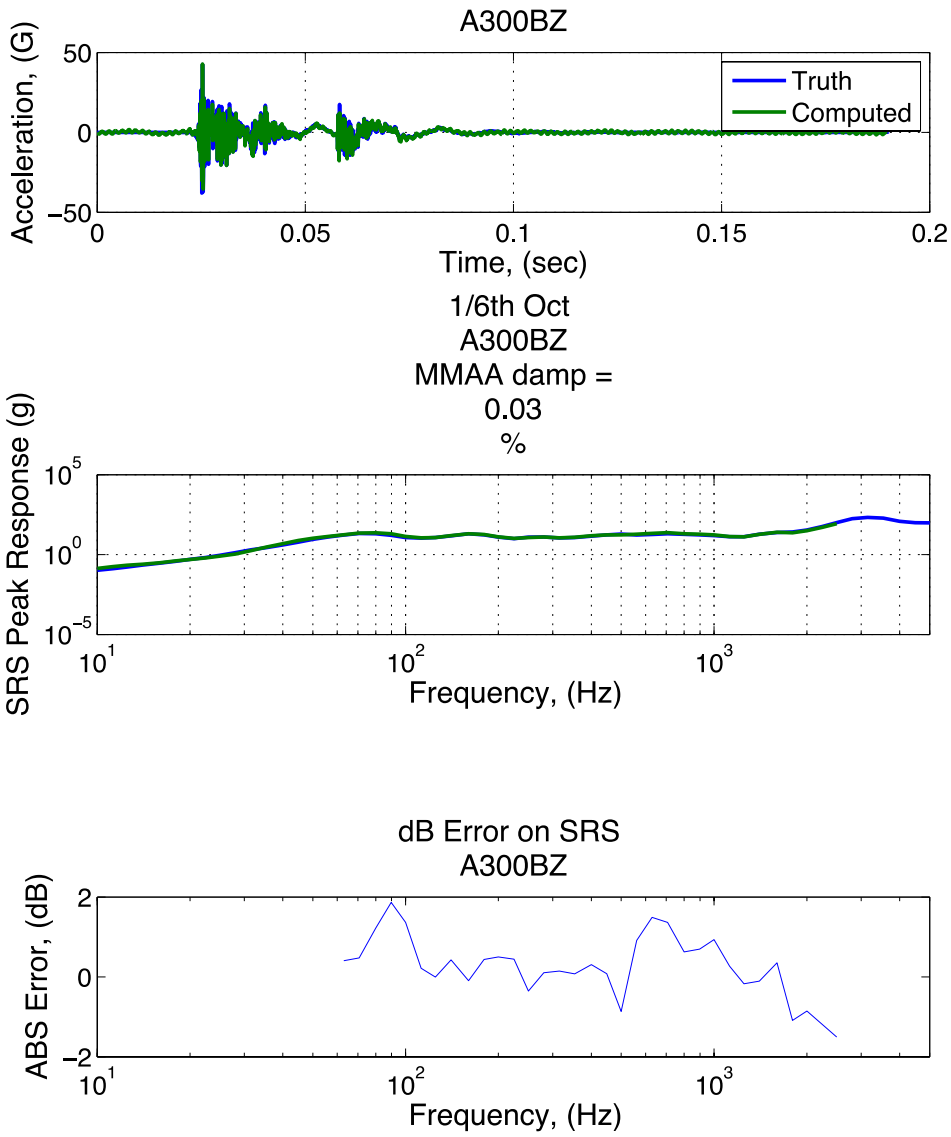

Figure 13: *Same Gage* comparison for gage 300BZ using the baseline set of gages.

1. Hammer Tip (High/Low Frequency)

From the hammer tap test, only two types of hammers were provided for comparison. The first is a high frequency steel hammer noted as (H1) and the second is low frequency yellow tip hammer noted as (H2). Given the baseline set of gages and using the *same gage* comparison, the high frequency hammer (H1) had a fairly large error of 9 *dB* at the low frequencies for the 601BZ gage location. The H2 hammer's largest dB error was 3.6 *dB* as previously mentioned. Therefore, the H2 was used for the remainder of this study. Intuitively, it is expected that the low frequency hammer would give better results for any gages not located on the outer skin of the system.

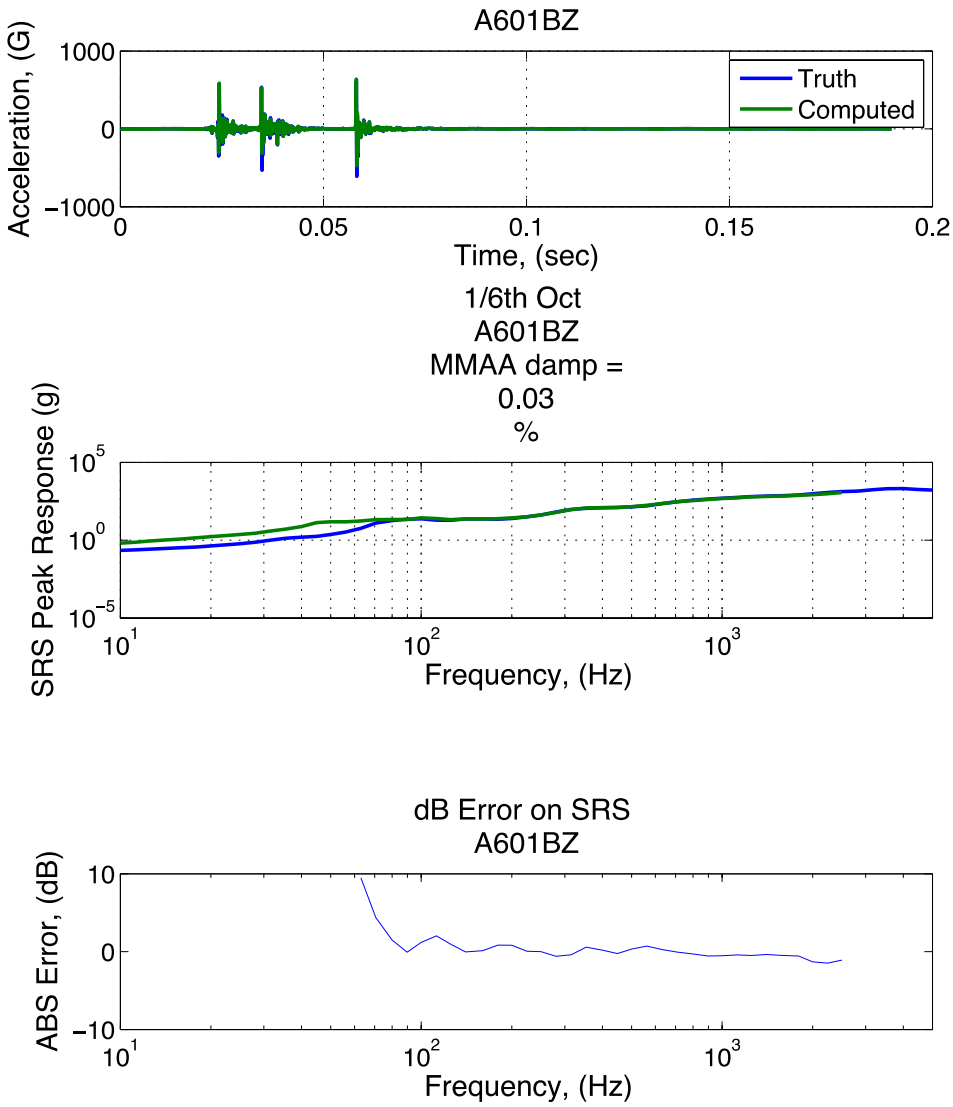

Figure 14: Gage 601BZ *same gage* comparison for high frequency hammer (H1).

2. Identification of Poor Gages for Inverse Problem

Before beginning the search for the optimal set of gages for force reconstruction, the list of gages were explored to see if there were any gages that would cause problems during the inversion process. For instance, a gage that went bad during either the ejection test or the hammer tap test would cause a significant error. To find the list of gages, the four previously mentioned gages, 601BZ, 100BZ, 110BZ, and 300BZ, were used and one additional gage was added to the list of gages for the force construction. The *same gage* comparison was then performed and if any 1/6th octave error increased above 20 *dB*, then the gage was removed from the overall list and identified as a bad gage. The process was obviously run until all gages were explored. The following list is the gages noted as bad for the particular hammer tap test and the ejection test at ambient temperature: 520BX, 109BZ, 201BY, 303BX, 361BZ, 410BZ, 420BY, 420BZ, 430BZ, 525BX, 610BX, and 635BZ. Figure 15 and Figure 16 illustrate the identification of the bad gages: 109BZ and 410BZ.

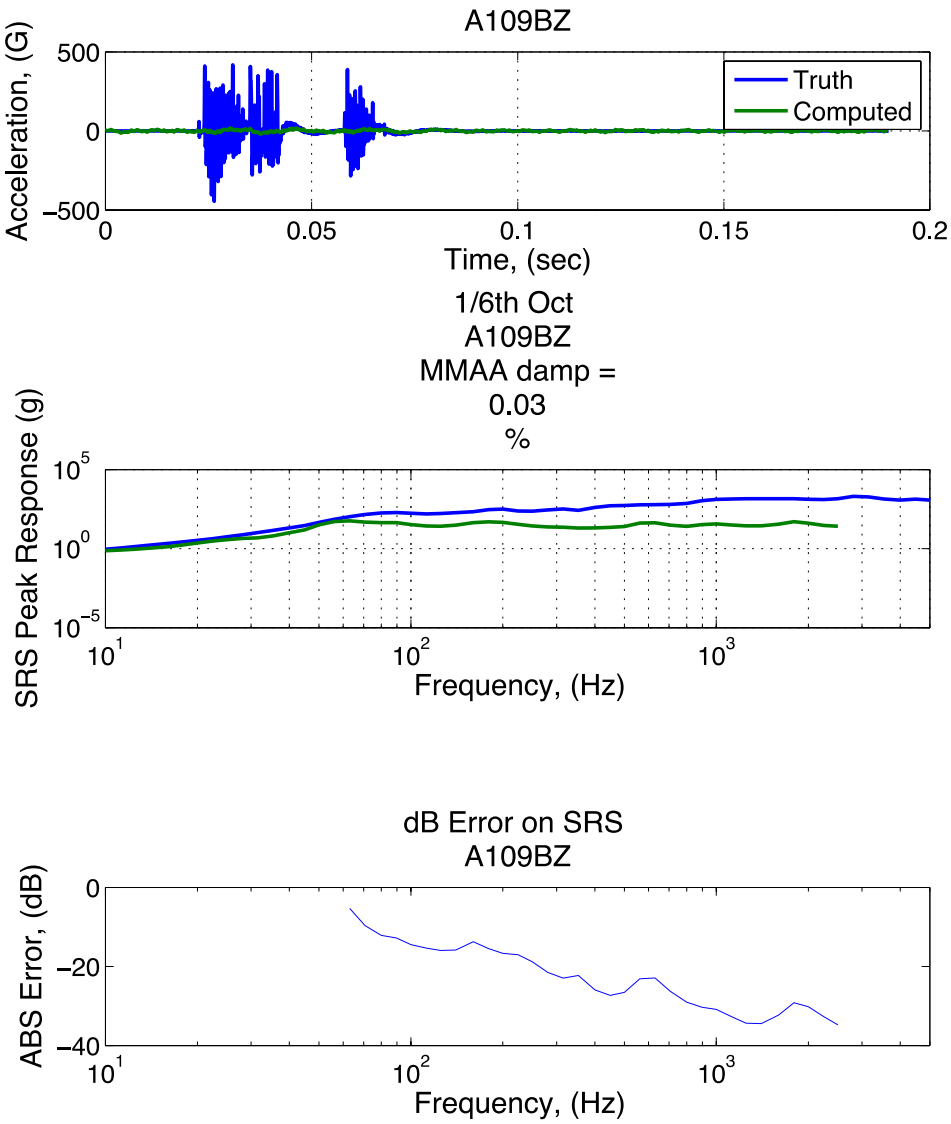

Figure 15: Identification of a bad gage 109BZ.

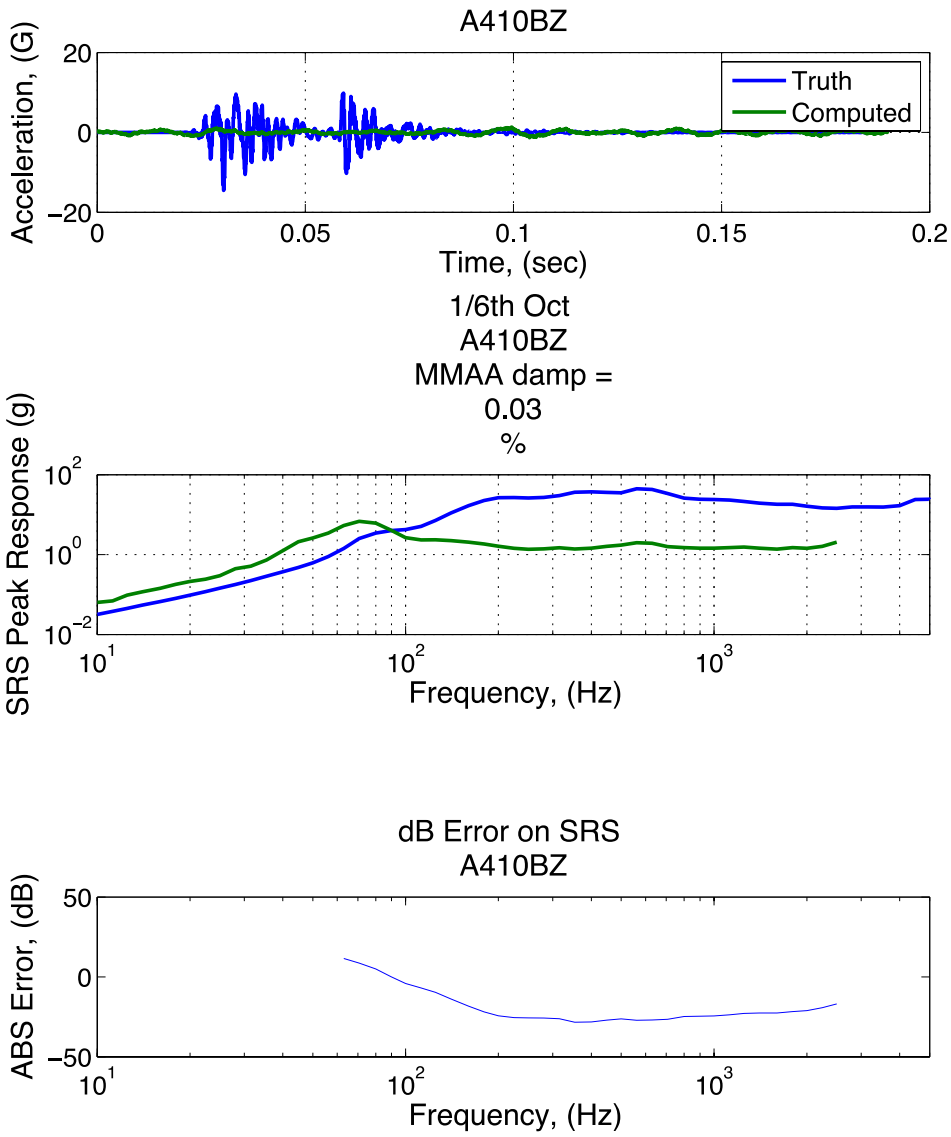

Figure 16: Identification of a bad gage 410BZ.

If we do the same procedure for all the ejection tests (a total of 33 tests including both hot and cold tests) and included any gages that were noted in any test notes as questionable, then we find the list of bad gages noted in Table 3.

Table 3: List of Bad Gages found for Ejection 1 Test Series that includes ambient, cold, and hot tests.

Bad Gage List		
'100BZ'	'400BX'	'471CZ'
'109BZ'	'400BY'	'500BX'
'120BZ'	'410BY'	'520BY'
'201BY'	'410BZ'	'601BY'
'202CX'	'420BX'	'609BZ'
'202CY'	'420BY'	'610BX'
'202CZ'	'420BZ'	'620BZ'
'300BX'	'430BX'	'625BZ'
'303BX'	'430BZ'	
'361BX'	'440BY'	

3. Gage Selection for Force Reconstruction

A simple sampling method was used to find an adequate list of gages to be used for the force reconstruction. The store has a body region that has gages that are difficult to excite due to various damping mechanism within that region. Therfore, it was a little unsure if that region's gages could be use for the inversion. Thus, two force reconstructions were conducted: one with including the body gages and one without. The sampling method selects a unique set of gages that can range from 8 gages to 36 gages, if including the ability to use gages within the body. If gages within the body are excluded from the analysis, then the range is from 8 to 23 gages, since after removing the bad gages and the body gages there would only be 29 gages left. These gages are randomly chosen. There were fourteen separate 1,000 iterations performed for a total of 14,000 random selections of sets of gages for the force reconstruction using the inverse method: $\{F(\omega)\}_{field1} = [H(\omega)]_{ham}^{-\dagger} \{A(\omega)\}_{field1}$. For all 14,000 perturbations the *opposite gage* and *check list* comparison is used. Recall that the *opposite gage* comparison uses the remainder of gages not used for the force reconstruction. During each iteration, the maximum 1/6th octave error is saved for each of the *opposite gages* and the *check list gages*.

The mean of the dB error's for each gage is used for evaluation of the randomly selected gages. The mean of the absolute errors for the *opposite gage* was found to be 5.0 *dB* with the set of gages listed in Table 4 if including body gages, and 4.5 *dB* for the *check list gages.* The mean of the absolute errors for the *opposite gages* was found to be 5.4 *dB* with the set of gages listed in Table 5 if excluding body gages, and 4.5 *dB* for the *check list gages*. Because of concern with the noise in any body gages it has been determined that it would be best to go forward with only using gages that exclude any gages in the body region. The *check list gages'* result figures of the best set of gages are presented in Appendix A for the case of excluding the body gages.

Table 4: Best gage selection for force reconstruction if using Body Cages.

Best Gages Including Body Gages				
'100BY'	'303BY'	'440BZ'	'525BZ'	'625BY'
'110BY'	'360BY'	'460BX'	'601BX'	'630BX'
'120BY'	'360BZ'	'460BY'	'601BZ'	'630BY'
'200BY'	'410BX'	'460BZ'	'610BY'	'635BX'
'301BX'	'440BX'	'500BY'	'620BX'	'635BZ'
'301BY'				

Table 5: Best gage selection for force reconstruction if excluding Body Cages.

Best Gages Excluding Body Gages			
'110BX'	'520BX'	'601BZ'	'625BX'
'110BY'	'520BZ'	'610BY'	'625BY'
'110BZ'	'525BX'	'610BZ'	'630BX'
'120BX'	'525BY'	'620BX'	'635BX'
'120BY'	'601BX'	'620BY'	'635BZ'
'510CX'			

4. Hammer Tap Location (Input Location for H)

In the previous section a set of gages were found for the use in the force reconstruction. It assumed that the best set of force inputs were all eight input locations. This section addresses that assumption.

In order to find the best set of force inputs, a sampling method is again used. In this sampling method, a random set of force inputs are chosen with a minimum of four locations and maximum of eight locations. Two sets of response/acceleration gages were used for the force reconstruction. The first set is the one found in the previous section and the second set is the *check list* gages. The *check list* comparison is used to assess the best combination of force inputs by finding the combination that produces the minimum mean error with the least maximum variation.

If using the *check list* gages for the force reconstruction, then the six gages listed in Table 6 produce the minimum mean error of 0.008 *dB*; however, there is a large variation with the largest error noted as 27 *dB*. If using the best gages found in the previous section, then the best force locations are all eight locations. This produces a mean error of 0.12 *dB* with the largest error noted as 16 *dB*. Because the variation is smaller for the best gages found in the previous section and using all force locations, it is selected as the ideal set.

Table 6: Ideal force location for force reconstructed with check list gages.

Check List Ideal Force	
'FL'	'FSBY-'
'AL'	'ASBY+'
'AP'	'ASBY-'

Table 7: Ideal force location for force reconstructed when considering minimizing the largest error in the check list gages.

Check List Ideal Force	
'FL'	'FSBY-'
'FP'	'FSBY+'
'AL'	'ASBY+'
'AP'	'ASBY-'

E. Force Reconstruction Results

The forces generated at each input location are shown in Figure 17, which is difficult to draw any conclusions from. However, by summing the forces in the Z and Y directions, see Figure 18, three distinct events can be seen. The figures were recreated with allowing the time span to be that of the test duration and not limiting it to the range of 0.018 to 0.08 seconds. The first is at 0.02 seconds where the lugs are released and the preload is released at the lugs and the sway braces. At 0.035 seconds the pistons impact the system and begin to push the system off of the

aircraft. Finally, at 0.06 seconds the pistons bottom out and a step function load is imposed on the system. These times are obviously related to the test data.

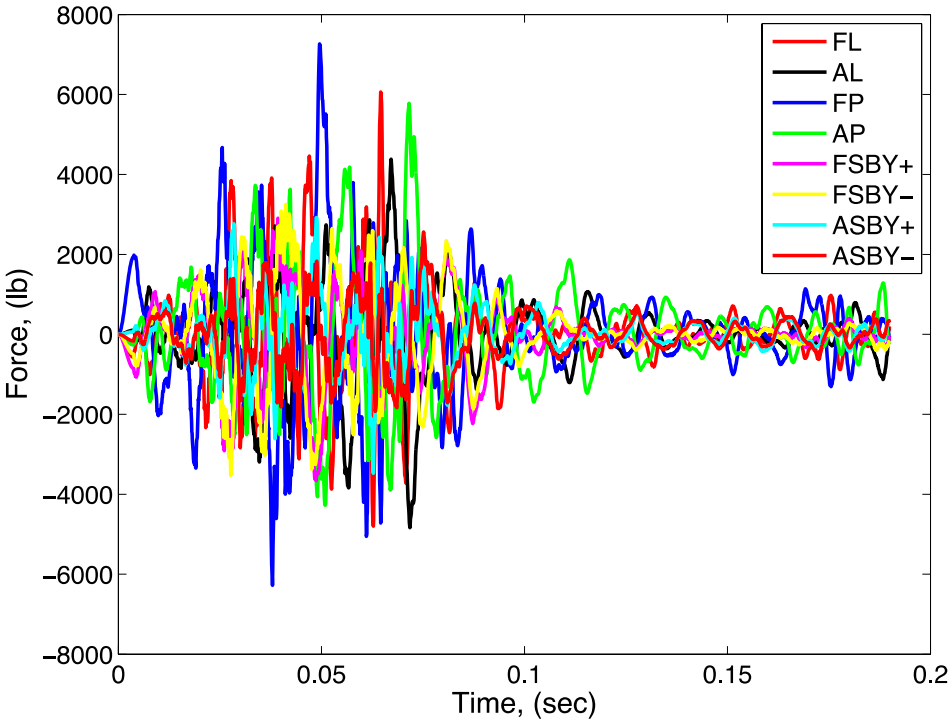

Figure 17: Best sampled generated forces at each of the input locations.

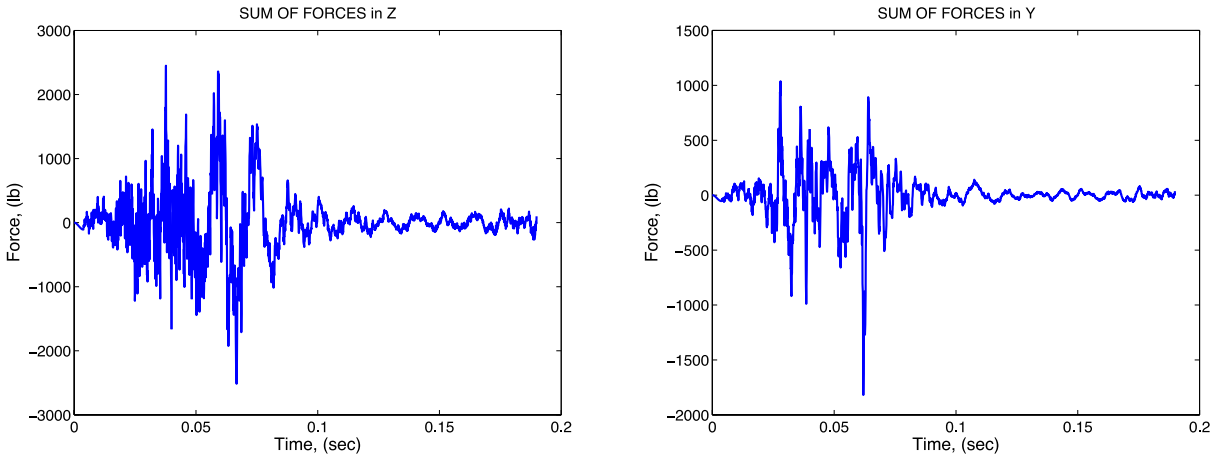

(A) Sum of Input Forces Z-Direction (B) Sum of Input Forces in the Y-Direction

Figure 18: Sum of the best sampled generated forces in the Z and Y directions.

III. Response of Missing Gages During Ejection Test

As long as the FRF matrix was formed with gages at desired locations, it in conjunction with the force that was reconstructed can be used to determine any desired gages response. This is beneficial for field tests where gages failed.

It is also possible that this could be used for a hammer tap test done on a different system; as long as the force reconstruction hammer tap system is the same as the field experiment. As an example, if a field test was performed

on a version "one" system and a hammer tap test was also performed on the version "one" unit, then a force vector could be generated with the method in Section II. If a hammer tap test was then performed on a version "two" system, then the force vector from version "one" field and hammer tap test could be used to generate responses for the version "two" system.

A. Low Frequency Haversine Pulse Addition

However, there is one minor detail that needs to be addressed. The force reconstruction was done with the acceleration data band pass filtered from 60-6,000 *Hz* and the matrix multiplication, $[H(\omega)]_{ham}^{-\dagger}\{A(\omega)\}_{field}$, done only on frequencies also from 60-6,000 *Hz*. However, there is frequency content below the 60 *Hz* low frequency cut-off. This frequency content was superimposed back into the excitation with the use of a haversine shaped pulse.

This needs to be performed because the hammer tap test lacked the low-frequency component, because the signals were high-pass filtered by the Data Acquisition System. Attempting to use the data below 60 *Hz* has resulted in significant error.

In order to get a relevant component response, a low frequency content will need to be added back into the system. This is accomplished with the use of the haversine shaped pulse:

$$A(t)_{hav} = \frac{1}{2}A_{peak}\left\{1 - cos\left(\frac{2\pi t}{T_{base}}\right)\right\}, \quad \text{for } 0 < t < T_{base}$$
$$A(t)_{hav} = 0, \quad \text{otherwise.} \tag{7}$$

By examining the data, T_{base}, was set to 0.045 *sec*. The peak acceleration, A_{peak}, was set by minimizing the error at 10 *Hz* and 20 *Hz* in the following manner. The set of best set of gages found in Section 3 was used for the force reconstruction. Then, the list of gages shown in Table 8 was run in the forward problem and the peak acceleration, A_{peak}, was found that minimized the error at 10 and 20 *Hz.* This produced a value of 24 *G* for the peak acceleration in the –Z direction. For this set of data the haversine pulse was started at 0.02 *sec*. The need for this addition is nicely shown in Figure 19 for gage 110.

Table 8: Gages used in forward problem for finding the peak acceleration needed for the haversine shaped pulse.

Z-direction Gages		
'100BZ'	'300BZ'	'601BZ'
'110BZ'	'301BZ'	'610BZ'
'200BZ'	'520BZ'	'620BZ'
'201BZ'	'525BZ'	'630BZ'

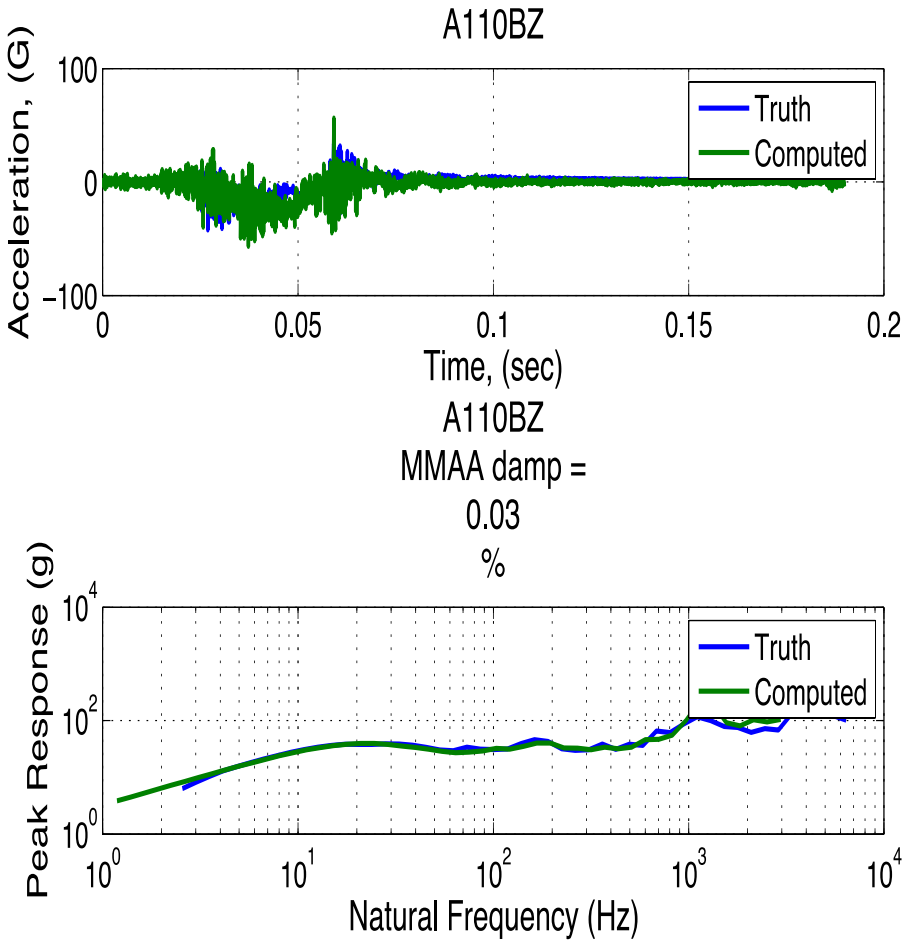

Figure 19: Low frequency haversine pulse added to computed gage 110 and compared to test data.

The negative Z-direction low frequency additional portion is understandable, because of the one-sided push off of the system. This push off is mainly symmetric; however, there is some low frequency content in the X and Y directions as well. Therefore, the same procedure was performed in these directions and it was found that a –X peak acceleration, A_{peakX}, of 0.4 *G*, and a –Y peak acceleration, A_{peakY}, of 1.2 *G* would minimize the 10 and 20 *Hz* error in these perspective directions.

B. Missing Gages 100, 500, and 601

As previously noted, this method can be used to fill in missing data from the field test due to bad gages. Three gages in particular were of concern: 100, 500, and 600. These gages did not fail during the ambient test and therefore a comparison to the ambient test is made in this section to validate the use of predictions for where the gages did fail. Figure 20 - Figure 22 depict the comparisons for these three gages. As can been seen, close agreement is made for all except gage 500 and only in the Y-direction. This particular gage (500BY) had significant problems during the cold and hot ejection test and it is quite possible that the gage was too damaged to provide a decent transfer function during the hammer tap test.

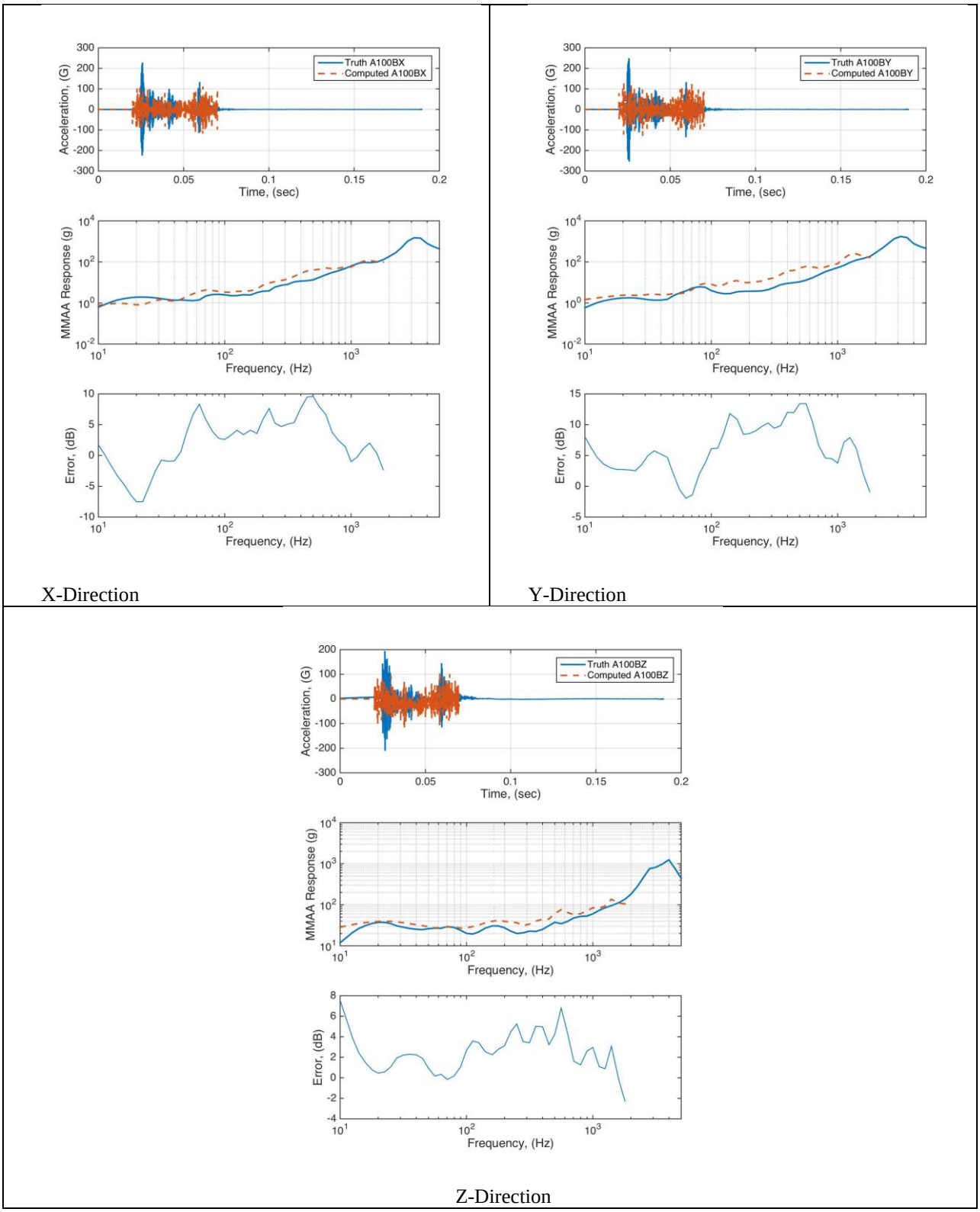

Figure 20: Gage 100 Response comparison to ambient ejection test for the best set of gages for force reconstruction.

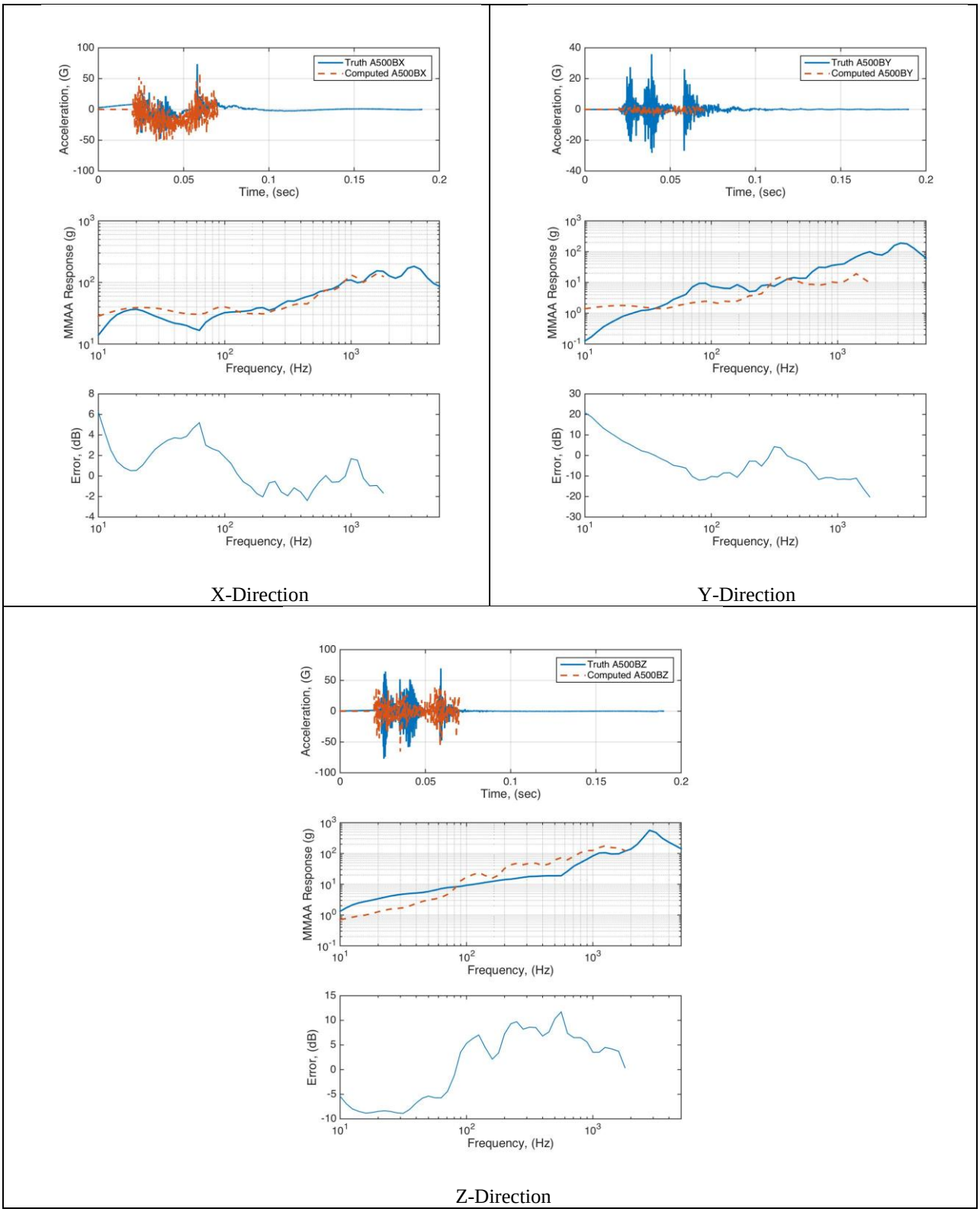

Figure 21: Gage 500 Response comparison to ambient ejection test for the best set of gages for force reconstruction.

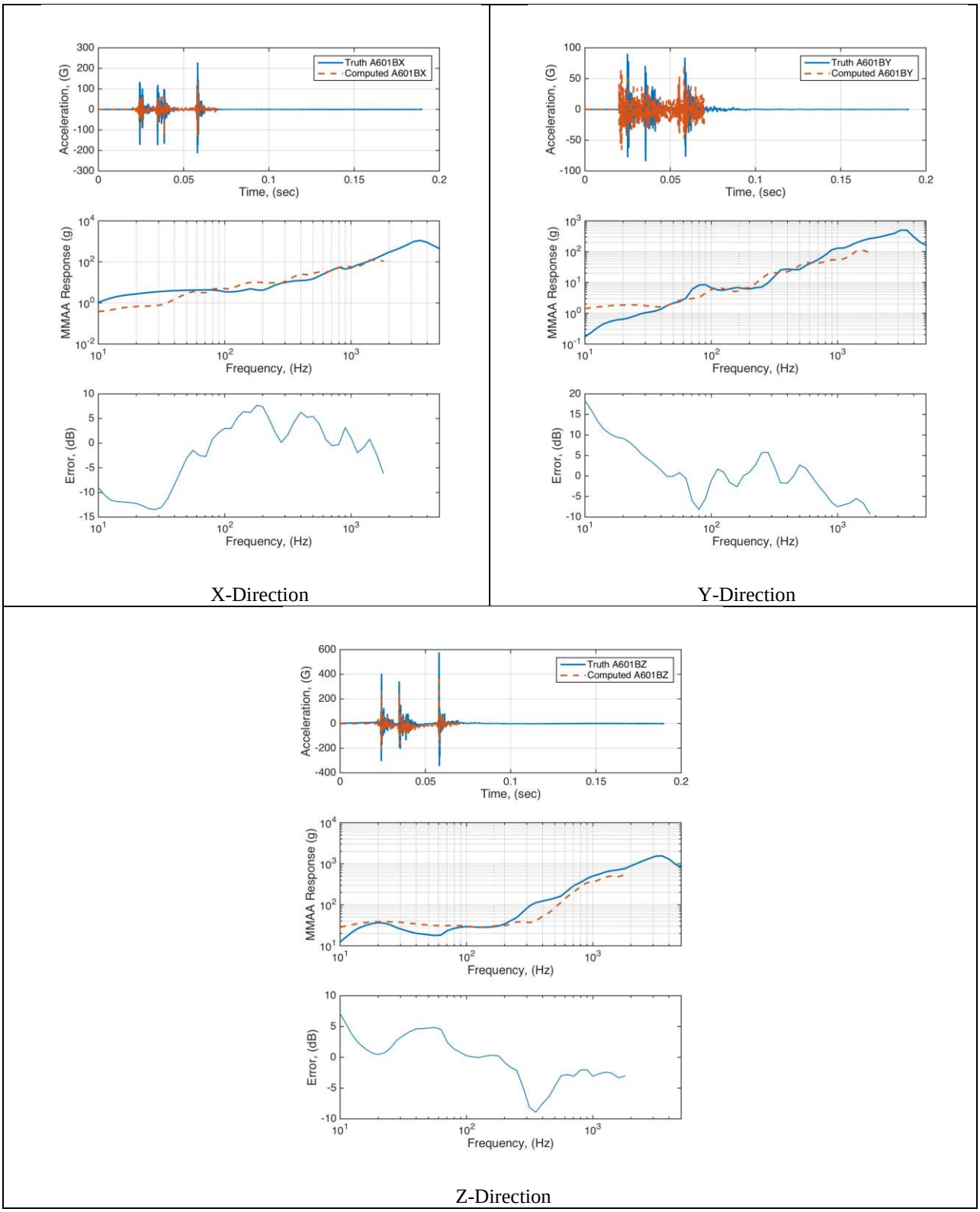

Figure 22: Gage 601 Response comparison to ambient ejection test for the best set of gages for force reconstruction.

IV. Experimentally Derived Model and Validation

Given the previous sections results, an experimental derived model (EDM) has been built for the ejection test series. The EDM is nothing more than the FRF matrix with the force input from the force reconstruction. Inherently, this model has some numerical error as well as model form error. As an example, the FRF matrix is formed from a hammer tap test that is at a lower level of excitation. The higher-level field experiments can have nonlinear effects that would not be captured with the lower level hammer tap test.

None-the-less, this model can be used to compare to other models and provide validation. As a metric for validation, the $1/6^{th}$ octave frequencies *dB* error for a particular gage can be used. There are 49 $1/6^{th}$ octave center frequencies between 10 and 2,500 *Hz*. Thus, each gage will have 49 $1/6^{th}$ octave *dB* error points for the frequency range of 10 to 2,500 *Hz*. A median and standard deviation can be computed for each gage based on these 49 frequency points. It in essence provides a method for assessing the overall accuracy across frequencies for a gage.

As an example, if we take the eject test data with the best sampled set of acceleration gages for the force reconstruction, generate the necessary force, and then run the forward problem to get all gage responses we have the median and standard deviation as shown in Figure 23. Observation of this data provides two clear insights. The first is that the method provides reasonable accuracy for all series of data except the 400 series. The second is that the method provides a very accurate method for Z-direction responses. All the Z-direction gages are provided in Figure 24. Care must be taken, because the gage title does not necessarily indicate the direction the gage was placed. In fact, the gage 460BX, which is supposed to align with the Z-direction axis is such an anomaly with the remainder Z-direction gages that it is questionable if it was truly in the Z-direction.

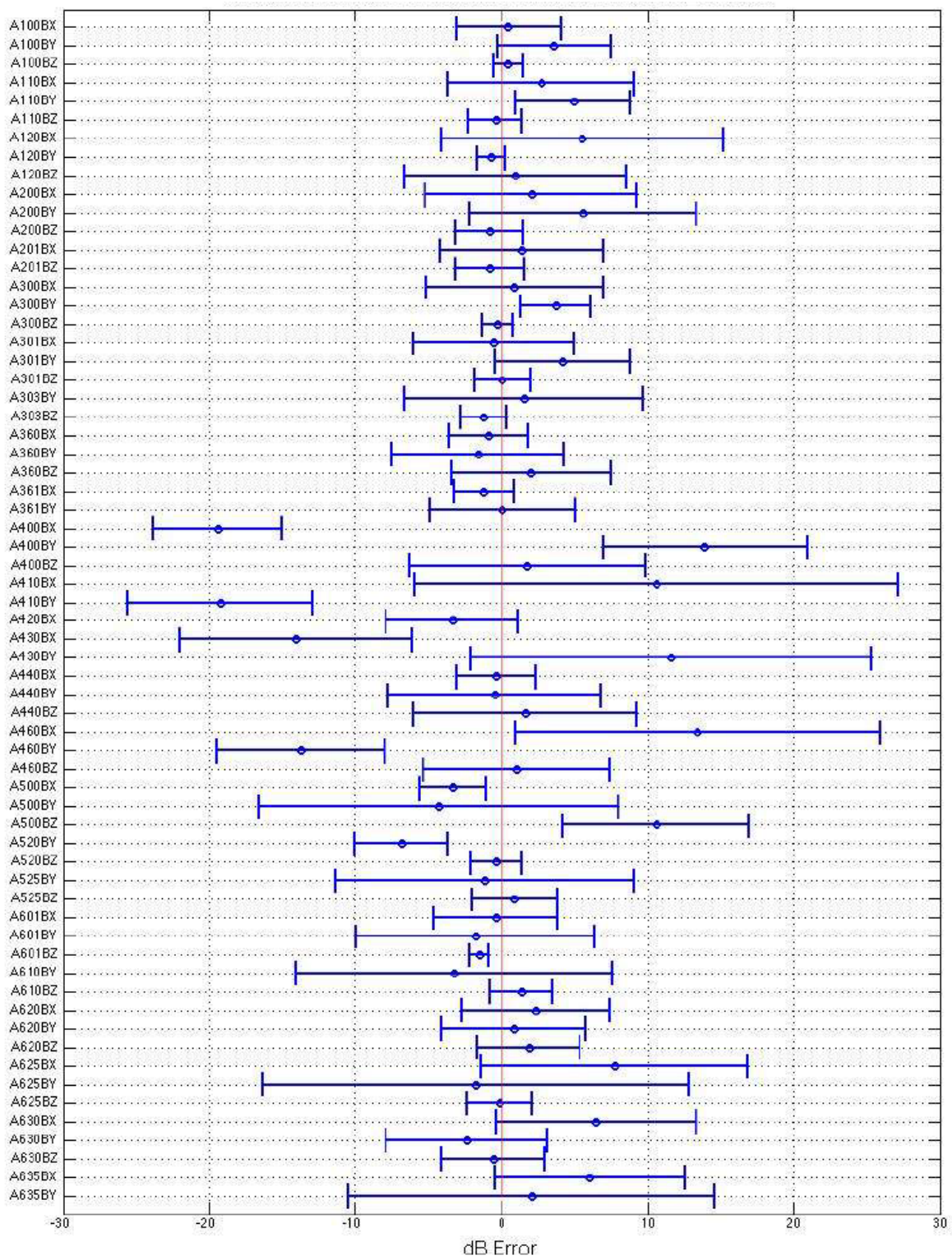

Figure 23: Mean and standard deviation of the 1/6th octave frequency errors for each gage of the ejection test.

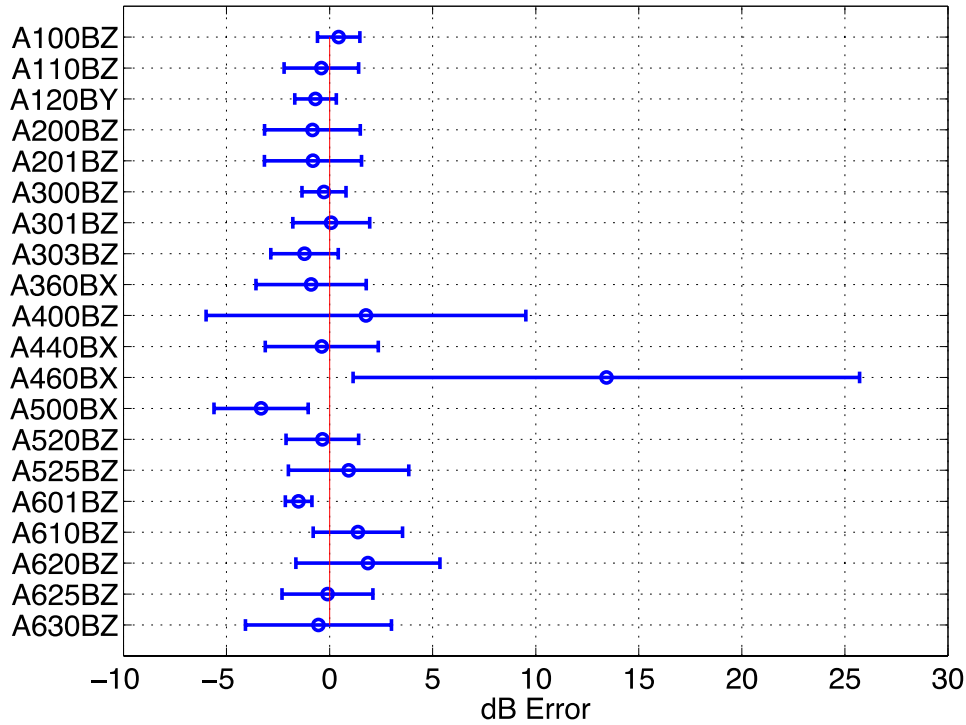

Figure 24: Mean and standard deviation of the 1/6th octave frequency errors for each gage in the Z-direction for the ejection test.

As a validation exercise, the best set of gages found in Section 3, is used for force reconstruction of a complete different ejection rack noted as *Rack B*. A comparison of the Z-Direction gages is shown in Figure 25 between the original, *Rack A*, force reconstructed component response and the *Rack B*. For all but one gage the *Rack B* responses are higher (the error is more positive). This is probably due to the use of the peak acceleration, 24 *G*, in the additional haversine pulse. This value was used for both the *Rack A* and the *Rack B*; however, the low frequency excitation of the *Rack B* probably needs to be explored and is less than the *Rack A*. None-the-less, the trend appears to be the same. In addition, the *check list* gages are compared between the *Rack A* and the *Rack B* in Figure 26, and there appears to be similar results. As a reminder a 6 *dB* error would be an indication of twice the amplitude.

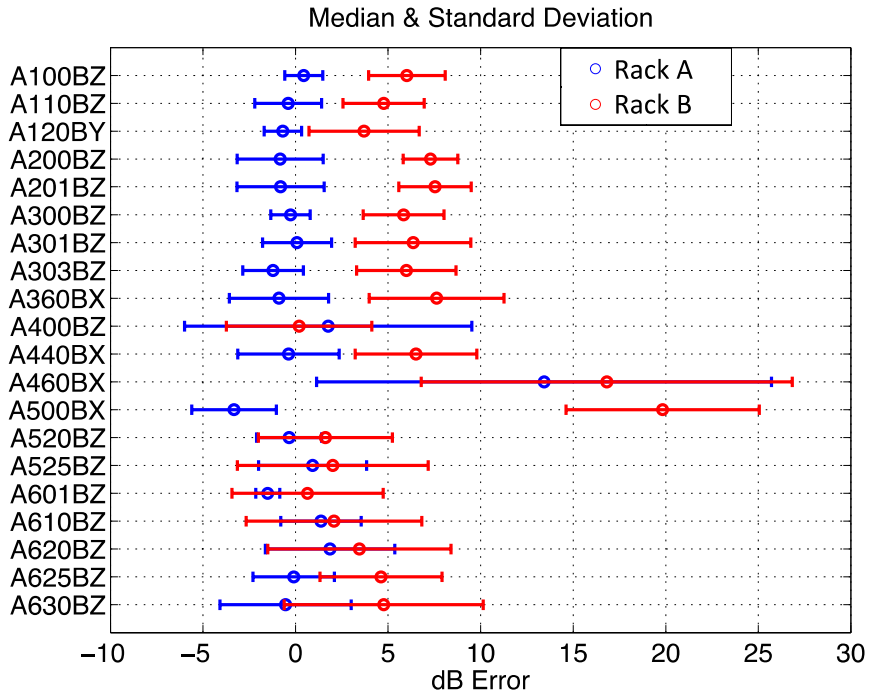

Figure 25: Z-Direction comparison of *dB* error for the Rack A & Rack B component responses.

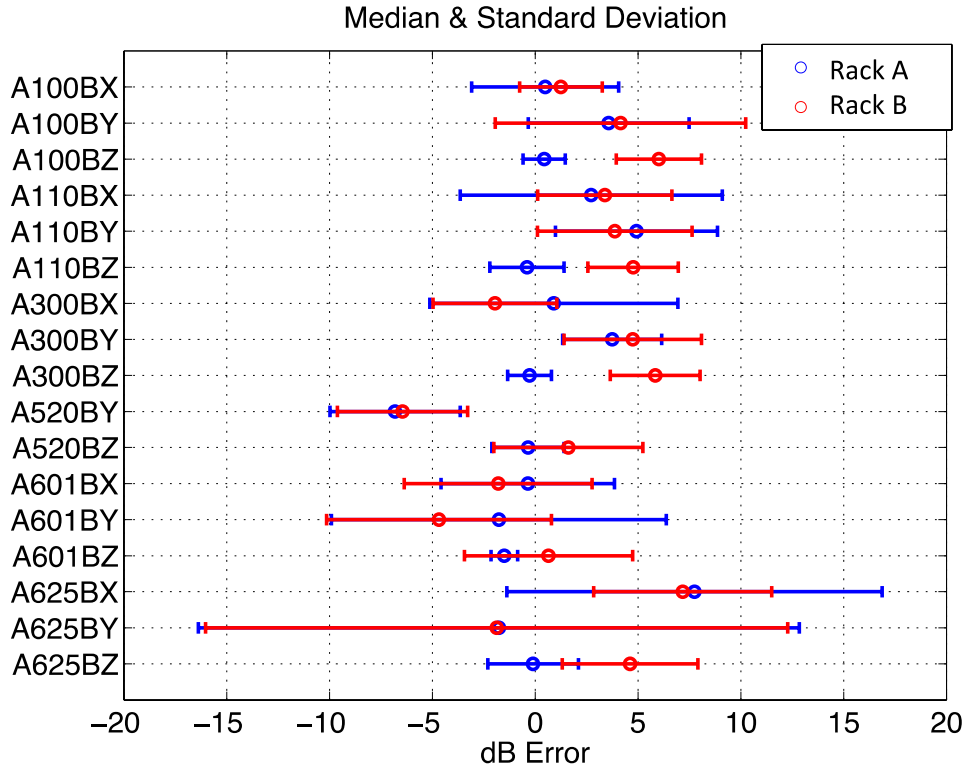

Figure 26: Comparison of *dB* error for the Rack A & Rack B using the *check list* gages.

V. Conclusion

This study has shown a method for developing inputs for a FE model and for replacing gages lost during a field ejection test. It uses a simple sampling method to find a preferred set of gages to be used for the force reconstruction. Verification of the code and algorithm is provided. The work concludes with a validation study for a different rack used for ejection.

Three particular locations during a recent ejection test were explored for reconstruction, since these areas had problems during the ejection test. It was found that the method could reconstruct eight of the nine gage responses. It is believed that the one it could not reproduce had problems during the experiment to formulate the transfer function.

A. Issues Found During the Analyses

Probably the biggest area of concern is that the gage noted orientation and polarity were not always correct. It is recommended that simple low level sine tests be performed on hardware if these methods are to be used in the future. A low level sine test would allow for the determination of gage orientations and polarities.

B. Future Work

This work could be improved with testing the following ideas. First, a high frequency hammer could be used to generate the high frequency response and a low frequency hammer could be used to generate the low frequency response. Second, more than likely, a different field test would produce a different optimal set of gages for the force reconstruction. This work only explored the force reconstruction of the one particular ejection rack set-up. This was decided since the ejection rack chosen has been noted as being the design driver of the ejection racks. The process should be explored for the remaining racks. Finally, the system was excited at a low level probably keeping it linear to form the transfer function. However, the true excitation is at a high level where nonlinearities begin to come into play. These nonlinear effects should be explored.

Appendix A: Check List Gage Figures

In this appendix, the comparison to the *check list gages* are made for the set of gages found to be best for both including and excluding the body gages.

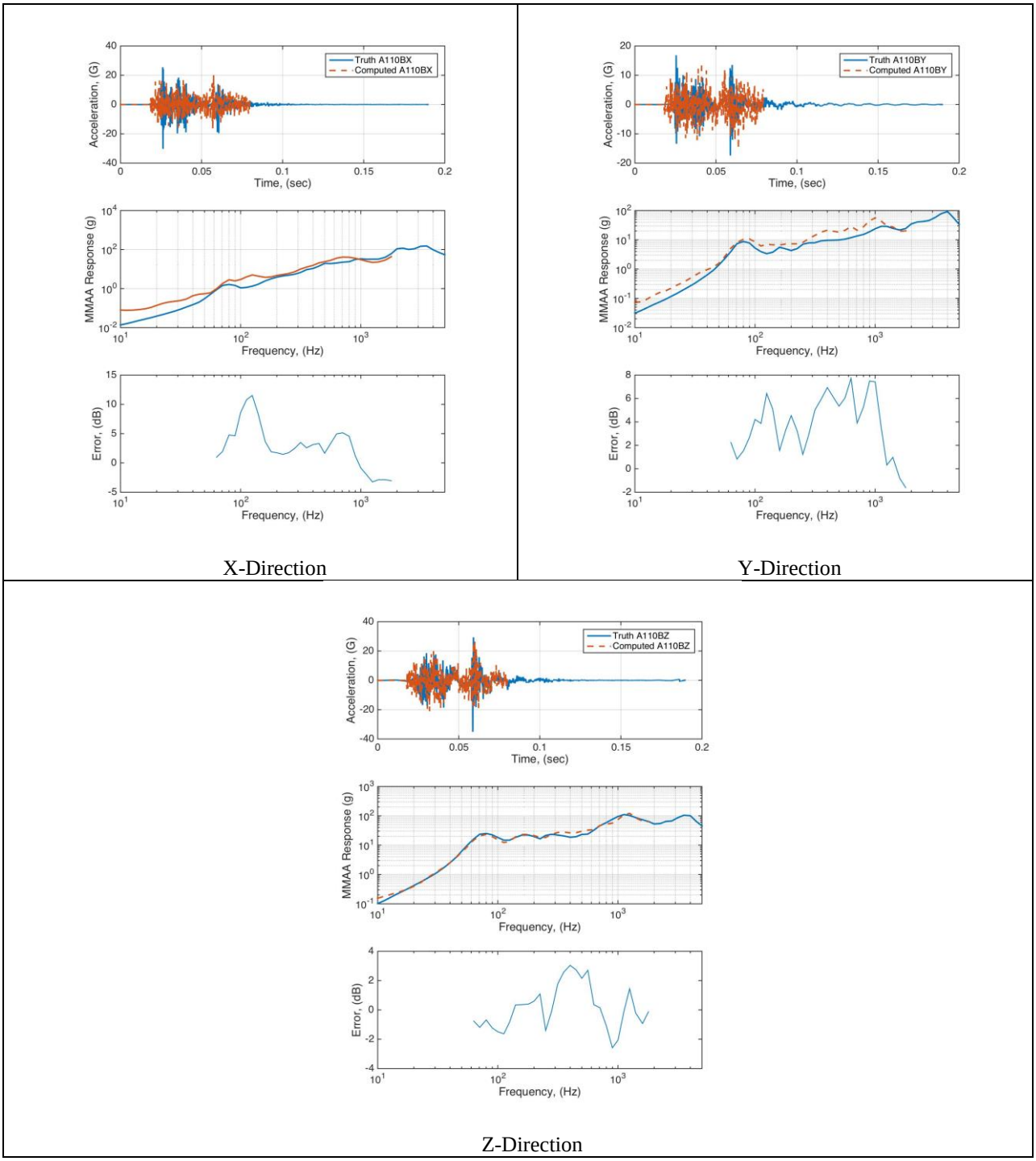

Figure 27: Check List Gage 110 for the best set of gages for force reconstruction.

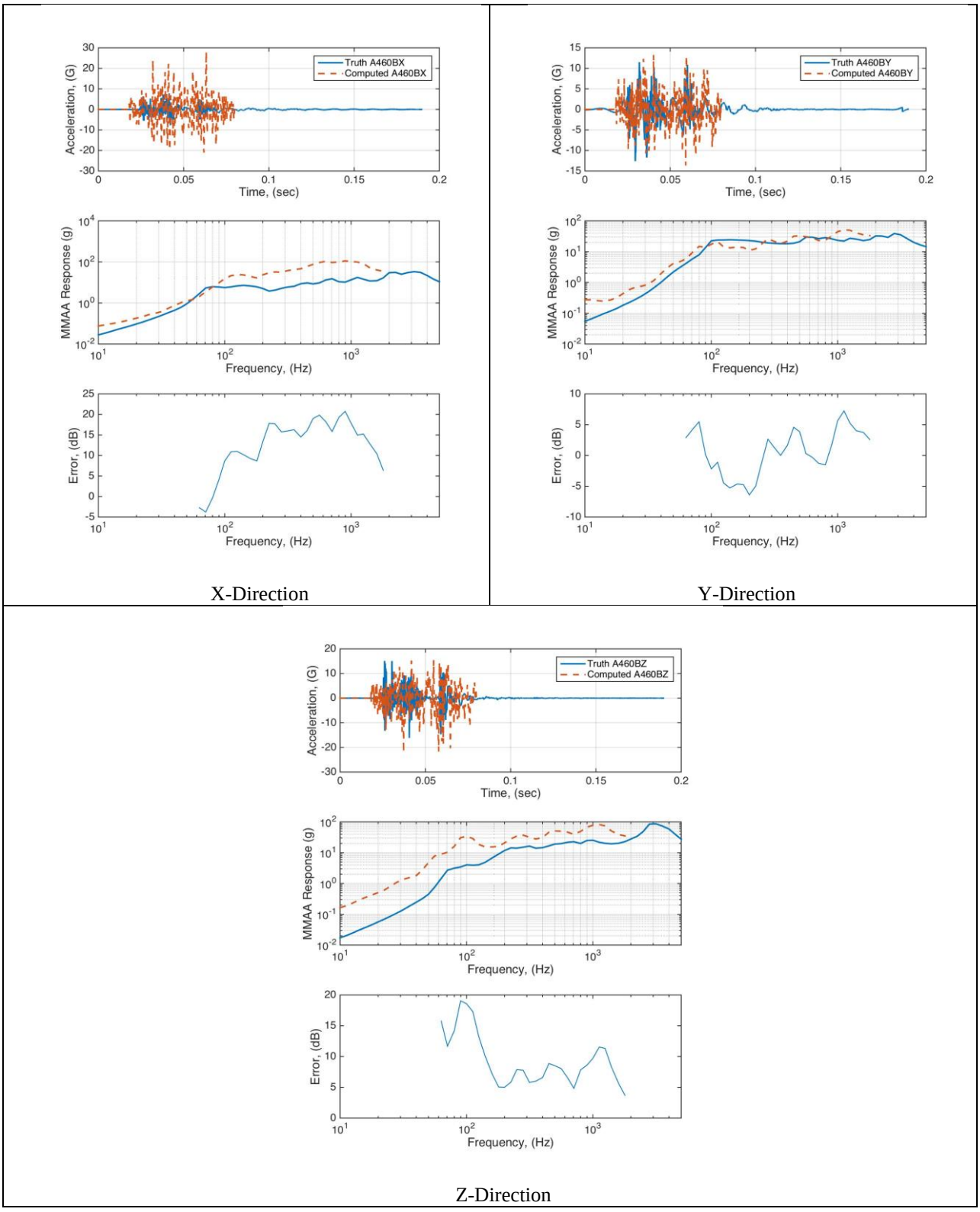

Figure 28: Check List Gage 460 for the best set of gages for force reconstruction.

This Gage went bad during the hammer tap testing.
X-Direction

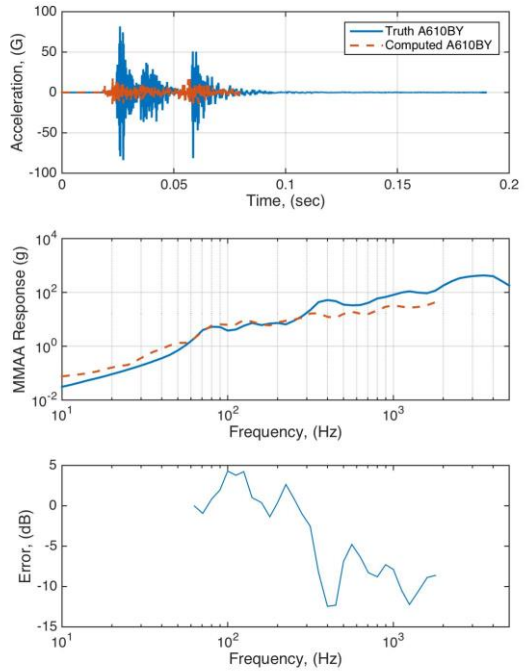

Y-Direction

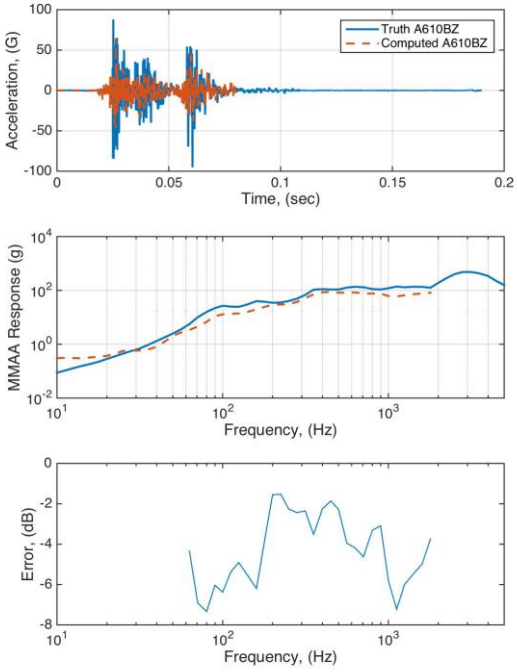

Z-Direction

Figure 29: Check List Gage 610 for the best set of gages for force reconstruction.

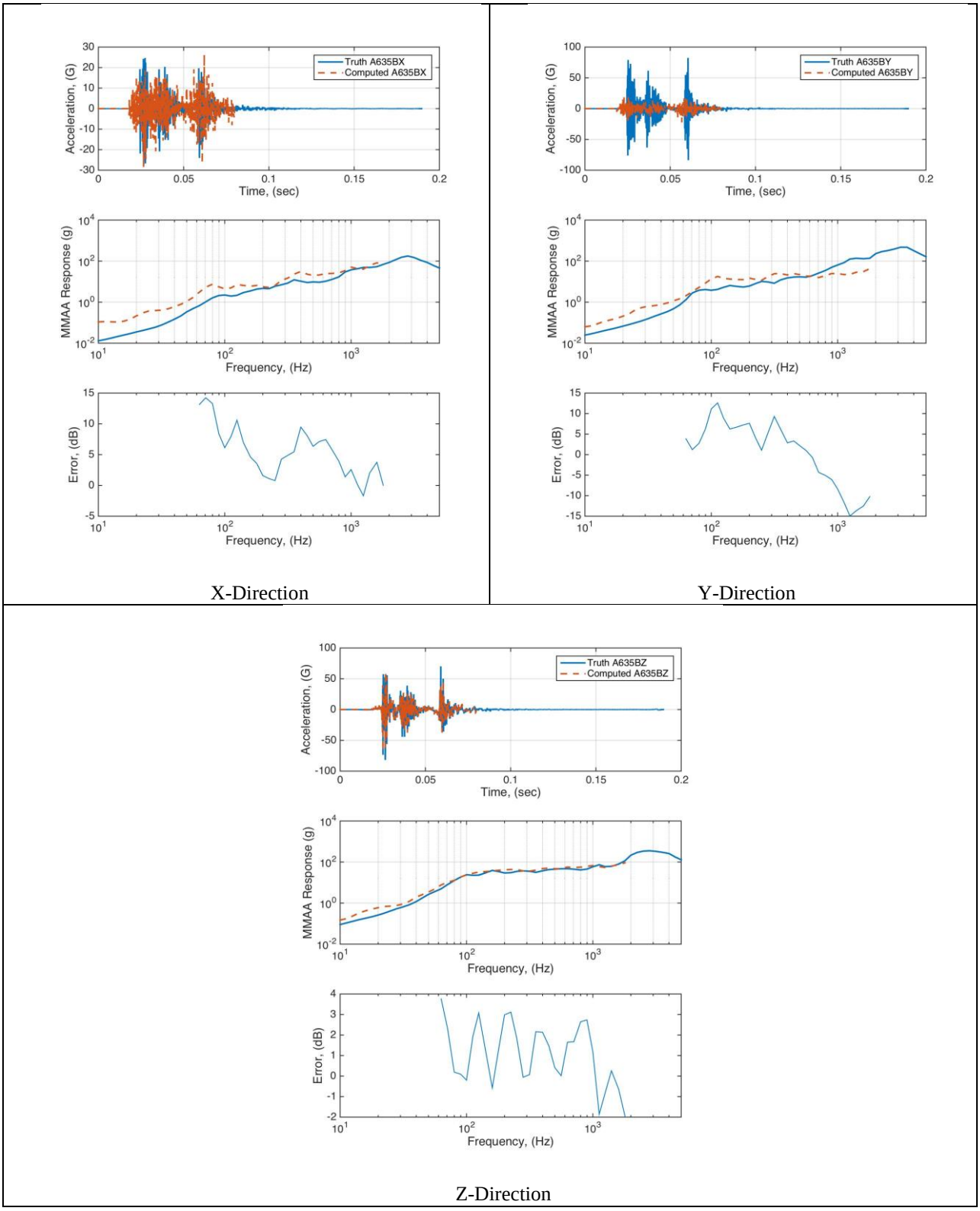

Figure 30: Check List Gage 635 for the best set of gages for force reconstruction.

Acknowledgments

Sandia is a multi-program laboratory managed operated by Sandia Corporation, a wholly owned subsidiary of Lockheed Martin Company, for the U.S. Department of Energy's National Nuclear Security Administration under Contract DE-AC04-94AL85000.

References

[1] P. H. Wirsching, T. L. Paez and K. Ortiz, Random Vibrations: Theory and Practice, New York, NY: Dover Publications, Inc. , 1995.

[2] AIAA, "Guide for the Verification and Validation of Computationl Fluid Dynamics Simulations," 1998.

[3] K. E. Atkinson, An INtroduction to Numerical Analysis, 2nd Edition ed., New York: John Wiley & Sons, 1988.

[4] D. Kincaid and W. Cheney, Numerical Analysis: Mathematics of Scientific Computing, 3rd Edition ed., B. Pirtle, Ed., Brooks/Cole, 2002.

[5] T. J. Baca, "Alternative Shock Characterizations for COnsistent Shock Test Specifications," *Shock and Vibration Bulletin*, vol. 54, pp. 109-130, 1984.

[6] D. O. Smallwood, "Characterizing Transient Vibrations Using Band Limited Moments," in *Proceedings of the 60th Shock and Vibration Symposium*, Portsmouth, VA, 1989.

[7] M. A. Biot, "A Mechancial Analyzer for the PRediction of Earthquake Stresses," *Bulletin Seismology Society of America*, vol. 31, 1941.